PNNL-14105

Pacific Northwest
National Laboratory
Operated by Battelle for the
U.S. Department of Energy

Feasibility Study on Using a Single Mixer Pump for Tank 241-AN-101 Waste Retrieval

Y. Onishi
B.E. Wells
S.T. Yokuda
G. Terrones

January 2003

Prepared for the U.S. Department of Energy
under Contract DE-AC06-76RL01830

DISCLAIMER

PACIFIC NORTHWEST NATIONAL LABORATORY
operated by
BATTELLE
for the
UNITED STATES DEPARTMENT OF ENERGY
under Contract DE-AC06-76RL01830

Printed in the United States of America
Available to DOE and DOE contractors from the
Office of Scientific and Technical Information,
P.O. Box 62, Oak Ridge, TN 37831-0062;
ph: (865) 576-8401
fax: (865) 576-5728
email: reports@adonis.osti.gov
Available to the public from the National Technical Information Service,
U.S. Department of Commerce, 5285 Port Royal Rd., Springfield, VA 22161
ph: (800) 553-6847
fax: (703) 605-6900
email: orders@ntis.fedworld.gov
online ordering: http://www.ntis.gov/ordering.htm


This document was printed on recycled paper.
(8/00)

PNNL-14105

Feasibility Study on Using a Single Mixer Pump for Tank 241-AN-101 Waste Retrieval

Y. Onishi
B. E. Wells
S. T. Yokuda
G. Terrones

January 2003

Prepared for
the U.S. Department of Energy
under contract DE-AC06-76RL01830

Pacific Northwest National Laboratory
Richland, WA 99352

Summary

The current waste retrieval plan calls for using two mixer pumps located 20 ft (6.1 m) from the tank center to mix waste stored in Hanford Tank 241-AN-101 (AN-101). The objective of this evaluation was to determine whether a single rotating 300-hp mixer pump located 20 ft (6.1 m) off-center could adequately mix the expected AN-101 tank waste.

Expected AN-101 waste is a mixture of the original 12-in.- (0.33-m-) thick AN-101 liquid waste, 40% in-line dilution of AN-104 supernatant liquid, and 43% in-tank dilution of AN-104 saltcake. Chemical modeling indicates that the $Na_2CO_3H_2O$, $NaNO_3$, Na_2SO4, and NaF in the AN-104 solids would dissolve, resulting in an 88% reduction in solids. For conservatism, we assumed that all remaining solids were collected in AN-101. Thus, the diluted waste to be stored in AN-101 would consist of an 18.9-in. (0.48-m) solids layer (at the original AN-101 solids volume fraction) and a 266.1-in. (6.76-m) liquid layer, totaling 285.0 in. (7.24 m) of waste.

To mobilize the remaining waste, the pumps must overcome yield strength and high viscosity and mix the solids with the overlying liquid waste. Because there are no measured rheology data on the expected AN-101 waste, yield strength estimates were based on other tank waste data. The yield strength is estimated to be less than 150 Pa and most likely less than 60 Pa. We selected yield strengths of 1, 5, 20, 60, 100, and 150 Pa as a parametric evaluation. We used the three-dimensional TEMPEST code to simulate AN-101 pump jet mixing with a single pump 20 ft (6.1 m) off-center for nine baseline and inverted pump cases. The baseline pump has the intake below the injection nozzles; the inverted pump has injection nozzles below the pump inlet.

Table S.1 shows the predicted amount of solids erosion and the average thickness of the solids layers that are not eroded for all nine cases. As indicated in the table, a single, 20-ft off-center mixer pump (either baseline or inverted) is predicted to mobilize the solids up to the farthest tank wall for yield strengths of 150 Pa or less. Because the yield strength of the AN-101 waste is estimated to be less than 150 Pa, the AN-101 pump mixing model results indicate that a single mixer pump would mobilize the bulk of the disturbed and diluted AN-101 solids.

Table S.1. Predicted AN-101 Solids Erosion by a Single Off-Center Pump

Pump Type	Yield Strength, Pa	Pump Operation Time, min.	Solids Erosion Amount, vol%	Remaining Solids Layer Thickness, in. (m)
Baseline Pump	1	20	100	0
	5	40	100	0
	20	40	85.1	2.8 (0.072)
	60	40	80.1	3.8 (0.096)
	100	110	79.5	3.9 (0.098)
	150	120	78.6	4.0 (0.103)
Inverted Pump	60	55	89.3	2.0 (0.051)
	100	75	86.1	2.6 (0.067)
	150	75	83.6	3.1 (0.079)

Contents

Figures

Tables

1.0 Introduction

The current waste retrieval plan calls for using two mixer pumps located 20 ft (6.1 m) off the tank center to mix the waste stored in Hanford double-shell tank (DST) 241-AN-101 (AN-101). The objective of this evaluation was to determine whether a single rotating 300-hp mixer pump located 20 ft (6.1 m) off-center could adequately mix the expected AN-101 tank waste.

Tank AN-101 is located in the AN Tank Farm of the 200 East Area on the U.S. Department of Energy's Hanford Site in southeastern Washington State. It is one of 28 double-shell tanks storing waste at Hanford. The tank currently contains 1 ft (0.33 m) of supernatant liquid (Galbraith et al. 2002). The current plan projects that the tank would receive inline and in-tank diluted Tank AN-104 waste in the years 2005, 2007, and 2008 (Orme et al. 2001).

Because there are no measured rheology data on the expected AN-101 waste, we developed and applied an AN-101 model with viscosity and yield strength. The study approach was to:

- Determine expected volume and waste properties, especially the viscosity and yield strength of AN-101 waste with available data
- Determine erosion amount of a single off-center mixer pump under several different rheology conditions by running a series of the AN-101 model simulations
- Determine the feasibility of using a single mixer pump in AN-101 based on currently available information.

Section 2 describes AN-101 tank waste chemistry with predicted chemical reactions for inline and in-tank dilution processes to determine the amount and type of waste that can be expected in AN-101. Section 3 describes the expected waste physical properties after waste dilution and pipeline transfer. The assessment of the pump jet mixing of the diluted AN-101 waste is presented in Section 4. The summary and conclusions are stated in Section 5, while cited references are listed in Section 6.

2.0 AN-101 Tank Waste Chemistry

The expected AN-101 waste is a mixture of the following (Galbraith et al. 2001):

- Original 0.33-m-thick AN-101 liquid waste [Tank Waste Information System (TWINS) database (http://twins.pnl.gov) on 2/4/0])
- 40% in-line dilution of AN-104 supernatant liquid with water (Orme et al. 2001)
- 43% in-tank dilution of AN-104 saltcake with water (Orme et al. 2001).

AN-104 has a 4.05-m-thick saltcake and 5.67-m-thick supernatant liquid (Wells et al. 2002). We determine the final AN-101 waste volume by conducting chemical modeling to predict the expected waste chemistry. We used the GMIN chemical code (Felmy 1995) to predict aqueous and solids dissolution/precipitation due to waste mixing.

We first reproduced the current AN-101 supernatant liquid chemical composition based on information from TWINS (http://twins.pnl.gov) with the GMIN code. As shown in Figure 2.1, the main aqueous chemical species are Na^+, OH^-, NO_3^-, NO_2^-, $Al(OH)_4^-$, K^+, CO_3^{2-}, Cl^-, SO_4^{2-}, PO_4^{3-}, F^-, with trace amounts of $Cr(OH)_4^-$, $H_2SiO_4^{2-}$, and Ca^{2+} in order of abundance in molality.

Predicted and measured AN-104 aqueous chemical concentrations are shown in Figure 2.2. Predicted and estimated (based on measurements) solids in the AN-104 saltcake are shown in Figure 2.3. Figure 2.2 shows the predictions matched TWINS measured values well. Figure 2.2 indicates that chemical species present in AN-104 are similar to those of AN-101 but are present in much higher concentrations. Solids present in AN-104 saltcake are $Na_2CO_3 \cdot H_2O$, $NaNO_3$, $Na_2C_2O_4$, Na_2SO_4, NaF, $Cr(OH)_3$, $Na_3PO_4 \cdot 12H_2O$, SiO_2, and $Ca(OH)_2$, in order of abundance.

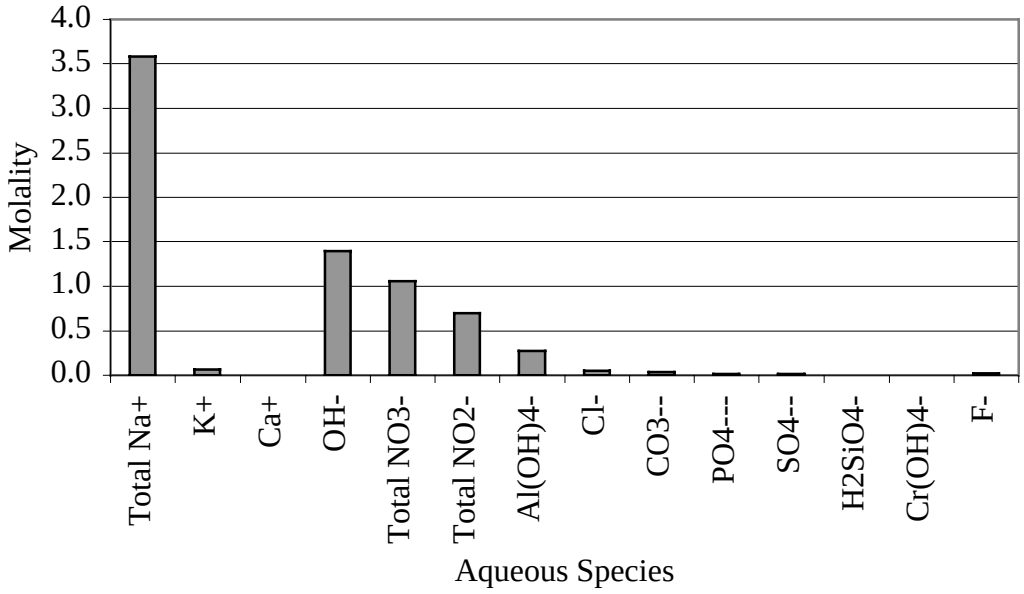

Figure 2.1. Current AN-101 Liquid Waste Chemistry

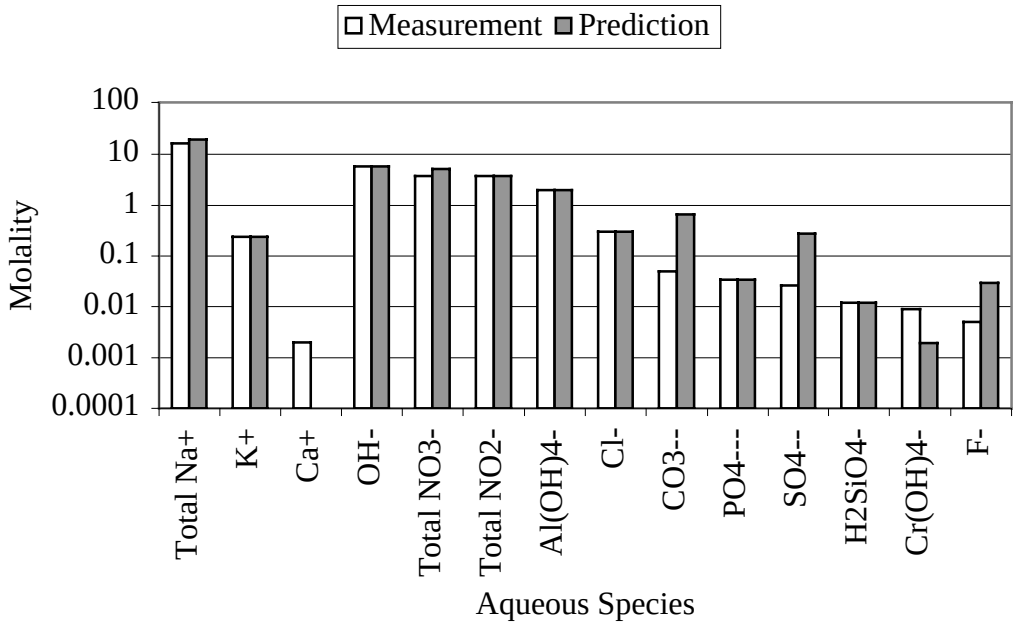

Figure 2.2. Predicted and Measured Current AN-104 Liquid Waste

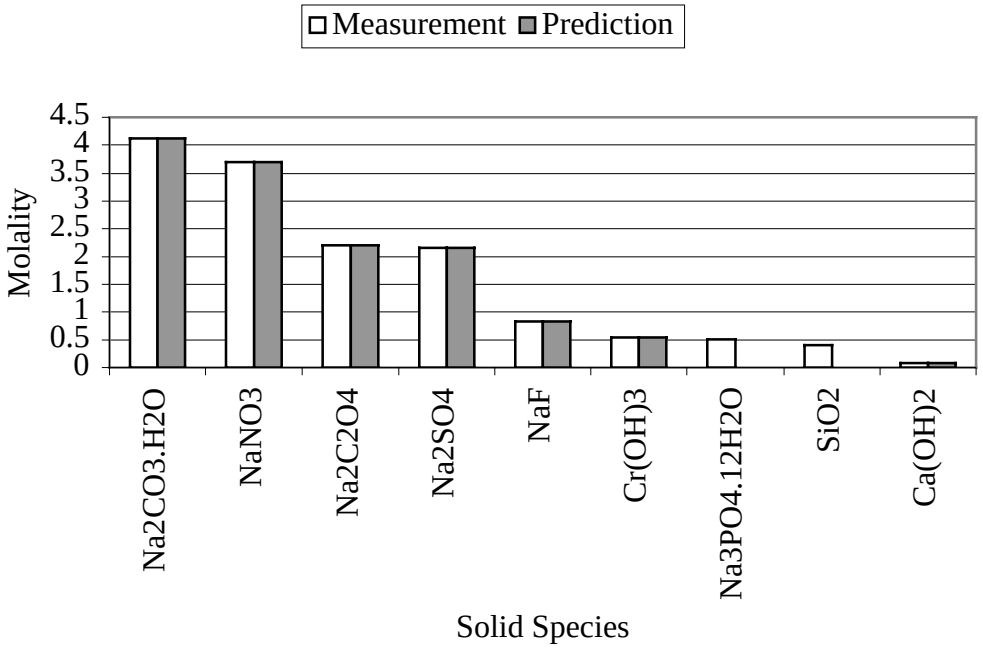

Figure 2.3. Predicted and Estimated (from measurements) Solids in Current AN-104 Saltcake

Predicted AN-101 liquid and solid wastes after mixing original AN-101 liquid waste and inline and in-tank diluted AN-104 waste with water are shown in Figure 2.4 and 2.5. As shown in these two figures, all $Na_2CO_3 \cdot H_2O$, $NaNO_3$, Na_2SO_4, and NaF solids in AN-104 s are predicted to be dissolved, resulting in an 88% reduction in molality in solid wastes.

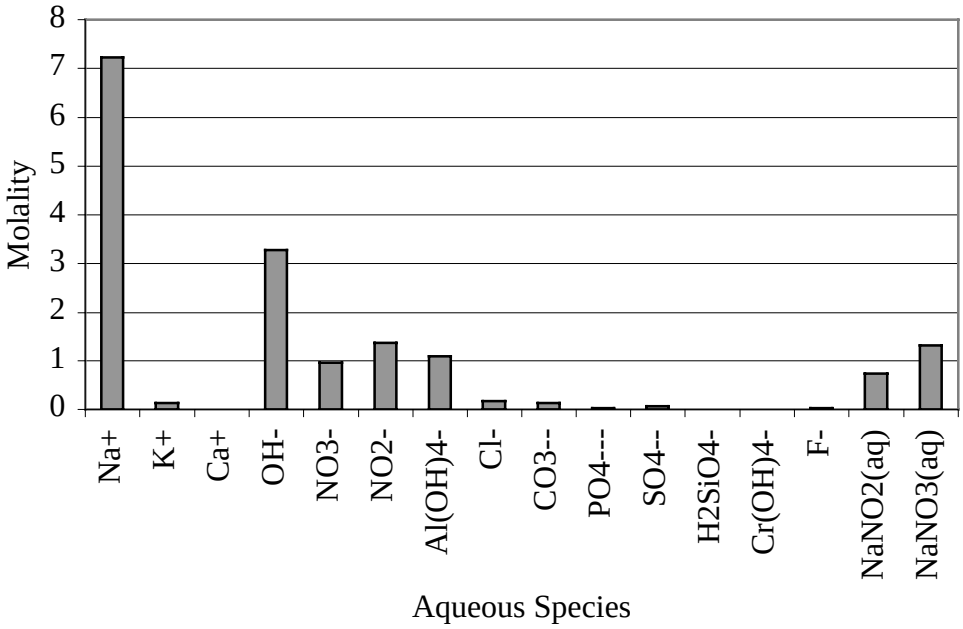

Figure 2.4. Predicted Final AN-101 Liquid Waste

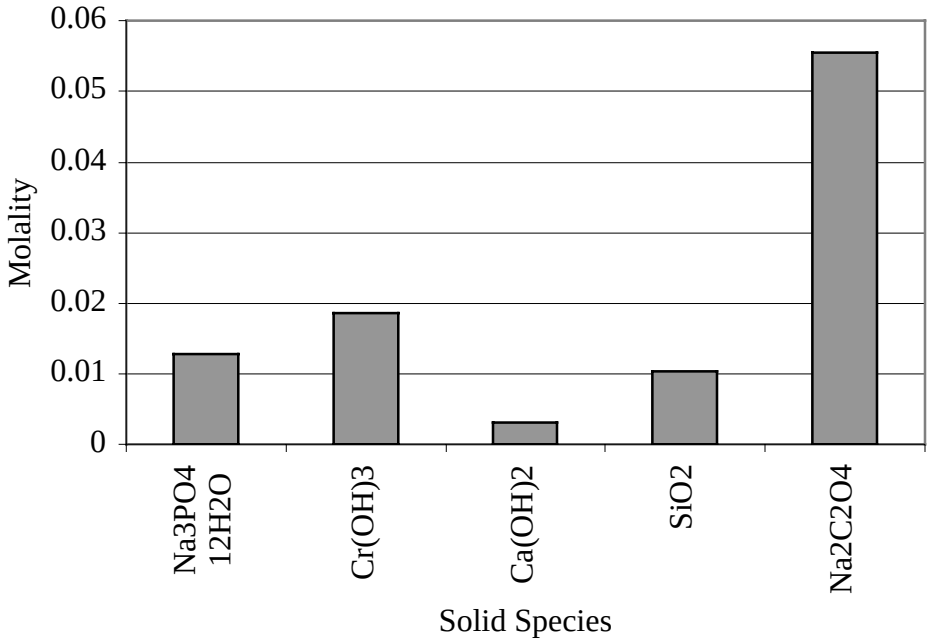

Figure 2.5. Predicted Final AN-101 Saltcake

3.0 Waste Physical Properties after Waste Dilution and Transfer

3.1 Expected AN-101 Waste Volume

Mixing AN-101 waste and inline and in-tank diluted AN-104 waste will dissolve 88% of the AN-104 solids, as discussed in Section 2. There are two mechanisms by which AN-104 solids could be transferred to AN-101. The first is a result of a spontaneous gas release process that would mobilize the solids during the AN-104 supernatant liquid transfer to AN-101. Section 3.3.4 describes the potential solids transfer during this transfer. The second mechanism is slurry transfer after the AN-104 saltcake has been diluted and mixed. Regardless of these two mechanisms, the final amount of the solids would be determined by the equilibrium chemistry of the mixture of the original AN-101 supernatant liquid waste and inline- and in-tank-diluted AN-104 waste. To be conservative for the amount of expected AN-101 waste and its properties, we assigned all the remaining solids to be in Tank AN-101, and while the total waste depth would be the same in Tanks AN-101 and AN-104. Thus, the diluted waste stored in AN-101 would consist of:

- an 18.9 in. (0.48 m) solids layer (at original AN-104 solids volume fraction of 16 vol%)
- a 266.1 in. (6.76 m) liquid layer
- 285.0 in. (7.24 m) total waste.

The AN-101 solids would be

- Solids dry mass = 66,100 kg
- Solids average density = 2,090 kg/m^3
- Saltcake thickness = 18.9 in. (0.48 m)
- Saltcake bulk density = 1,430 kg/m^3
- Solids volume fraction = 16 vol% (original AN-104 solids volume fraction).

In this assessment, the sizes of the expected AN-101 solid particles were assumed to be the same as those of the original AN-104 waste (Herting 1998). Four solid sizes were assumed for AN-101: 2, 12, 30, and 40 μm. The volume fractions of these four sizes are shown in Table 3.1.

Table 3.1. Expected AN-101 Waste Solid Sizes and Their Volume Percent

Solids Size Fraction	Solids Diameter, μm	Solids Volume Fraction, Vol%
Solid Size 1	2	6.57
Solid Size 2	12	2.71
Solid Size 3	30	4.65
Solid Size 4	40	2.07
Total		16.00

The expected AN-101 supernatant liquid would be

- Liquid mass = 8,246,900 kg
- Liquid density = 1,310 kg/m^3
- Liquid thickness = 266 in. (6.76 m).

3.2 Waste Viscosity

The AN-101 slurry (a mixture of the solids and supernatant liquid) was assume to change with the solids concentration and strain rate, and would be represented by the following AN-104 viscosity variation:

$$\mu(\dot{\gamma}, C_v) = \mu_N \, exp\left(A(\beta)\left\{1 + a_1\left[1 - \frac{2}{\pi} arctan\left(a_2 \, ln\, \lambda\dot{\gamma} + a_3\right)\right]\right\}\right) \tag{3.1}$$

where

$$A(\beta) = \frac{a_4\,\beta(1+4\beta)}{1 - a_5\,\beta\left(1 - 2\beta + a_6\,\beta^2\right)}, \text{ and } \beta = \frac{C_v}{C_{vm}}$$

a_i: = constants, as
- a_1 = 6.36
- a_2 = 0.64215
- a_3 = 4.15450
- a_4 = 0.55173
- a_5 = 3.14210
- a_6 = 0.62
- C_v = solids volume fraction
- C_{vm} = maximum solids volume fraction = 0.2
- μ = viscosity (in Pa-sec)
- μ_N = viscosity of the liquid = 0.0027 Pa-s
- λ: = time constant of the fluid = 0.01 s.

Note that AN-101 viscosity was assumed to have the same functional relationship as that of the AN-104 waste, but not the same viscosity value. The upper plot of Figure 3.1 shows this equation, together with measured viscosity values (Stewart et al. 1996; Herting 1998) used to develop this viscosity model. The lower plot shows viscosity behavior with solids concentration and strain rate. This viscosity expression was implemented to the TEMPEST code (Onishi and Trent 1999) to build the AN-101 model.

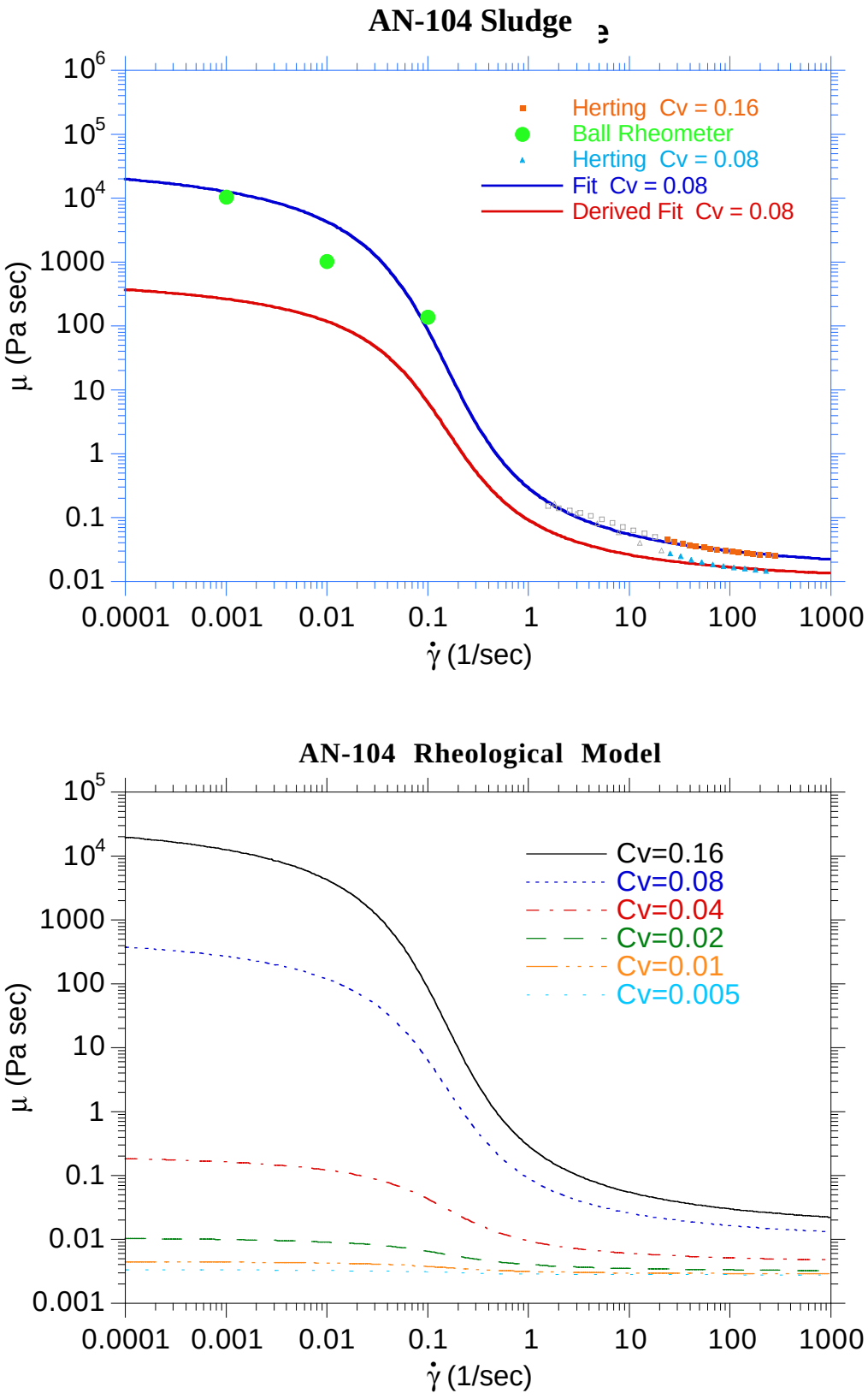

Figure 3.1. Variation of Viscosity of AN-104 Waste Used for AN-101 Model

3.3 Estimation of AN-101 Waste Yield Strength

The ability of a single 300-hp mixer pump to mobilize all of the predicted solids layer in Tank AN-101 after water dilution and mixing with AN-104 waste (presented in Section 2) was evaluated using the TEMPEST computer code (Onishi and Trent 1999). A significant parameter in this evaluation is the yield stress in shear of the solids layer.

AN-101 waste would be disturbed and diluted. Given that the AN-101 solids layer is a predicted entity, no experimental or in situ data are available. The yield stress of the predicted layer is therefore estimated based on its history and chemistry. We evaluated the potential effects of disturbance and dilution on the waste yield strength with the following information:

- AN-104 data
  - In situ yield strength measurements
  - Herting's dilution experiments
- AN-105 data
  - In situ yield strength measurements
  - Herting's dilution experiments
- Other direct yield strength measurements
  - SY-101
  - SY-103
- Comparison with waste chemistry
  - AZ-101
  - AZ-102
  - Other tank wastes

In Section 3.3.1, the response of AN-104 solids and other Hanford wastes to disturbance is presented. The effects of dilution on assorted Hanford wastes are examined in Section 3.3.2, and the predicted waste chemistry is compared with that of other wastes with measured yield stress in shear in Section 3.3.3. Suggestions are made in Section 3.3.4 for applicable values of the yield stress in shear of the predicted AN-101 solids layer.

3.3.1 Effect of Disturbance on the Yield Stress in Shear of Solids Layers

The effect of disturbing or mixing on the yield stress of a solids layer has been observed experimentally as well as in situ. Measurements in AN-104 are considered as well as those in other Hanford wastes.

3.3.1.1 AN-104 Yield Stress with Disturbance

In situ rheological measurements with the ball rheometer were conducted in AN-104 in early 1996 (Stewart et al. 1996). The ball rheometer was deployed through risers 16B and 1B, and repeated measurements were taken in each riser. The yield stress as a function of elevation above the tank bottom (solids layer depth in AN-104 is approximately 405 cm) is shown in Figure 3.2 for riser 16B and Figure 3.3 for riser 1B. The variation with depth may suggest that

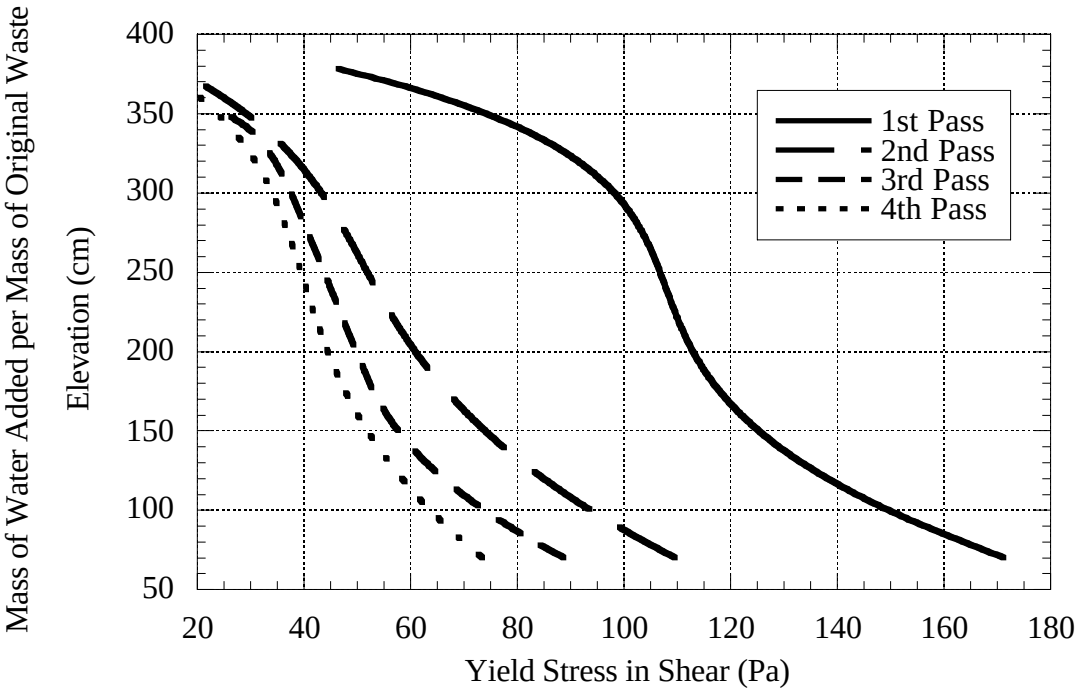

Figure 3.2. Yield Stress in AN-104 from Ball Rheometer, Riser 16B

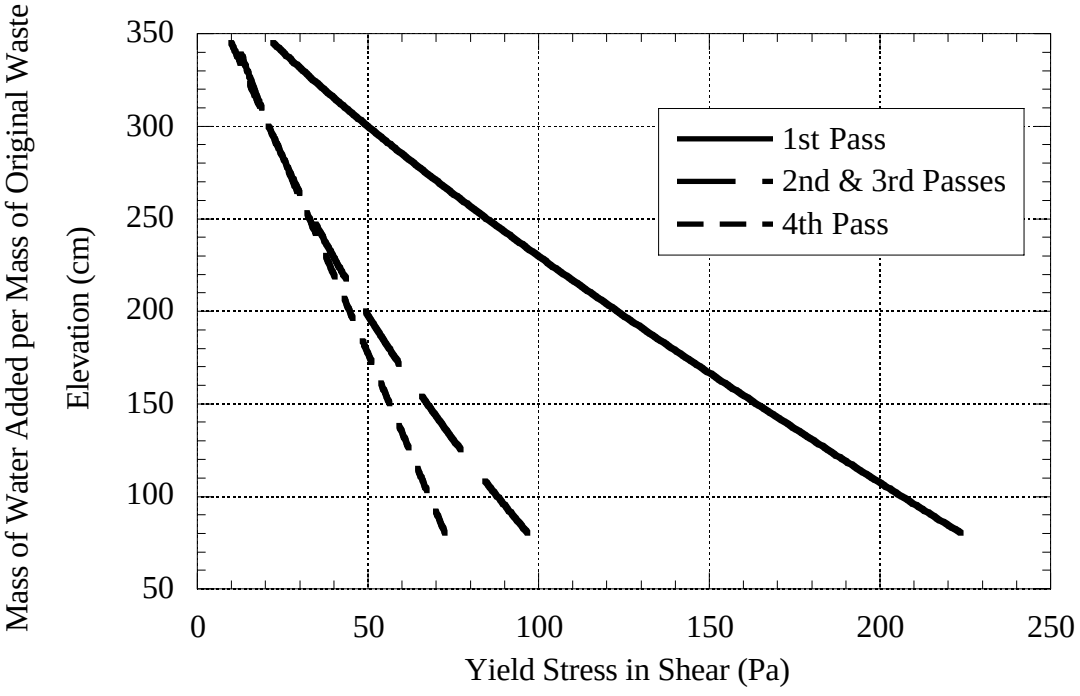

Figure 3.3. Yield Stress in AN-104 from Ball Rheometer, Riser 1B

lithostatic loading affects the yield strength. The yield stresses were recomputed from the 1996 data with higher precision and a correction for the actual ball speed during measurements. These improvements in the computations resulted in slightly higher values for the yield stresses in riser 16B than those reported earlier (Stewart et al 1996). Data for the second and third passes in riser 1B were difficult to discern from one another (the standard deviations overlapped), and were therefore combined. The time between passes is at least 50 minutes.

It is apparent that the yield stress is affected by waste disturbance. The average yield stress in the solids layer reduces by greater than a factor of two, and the yield stress appears to approach a minimum limit (≤50 Pa) asymptotically with repeated disturbances. Note that in this case the repeated disturbances are the passes of the ball rheometer and therefore may not represent the effect that solids mobilization by mixing may achieve.

Rheological measurements were taken in the laboratory on settled solids samples from AN-104 (Herting 1998). The samples were disturbed extensively before the measurements were taken, as will be described. The settled solids samples were prepared by taking representative samples (in proportion to their amounts in the tank) from the supernatant liquid and solids layer, and forming a whole-tank-composite. This whole tank composite was then well mixed and divided into subsamples, some of which were allowed to settle for six days, after which the supernatant liquid was decanted. The yield stress in shear of the samples was measured with a Haake viscometer at varied temperatures as a function of strain rate. In no case was any yield stress in shear identified. Given that the waste has yield strength in situ (measurements, gas retention behavior, etc.), the disturbance that the sample underwent was sufficient to negate this. This disturbance and resettling may be representative of solids mobilization by mixer pump(s).

3.3.1.2 AN-105 Yield Stress with Disturbance

In addition to AN-104 data, in situ measurements with the ball rheometer were also taken in AN-105 (Stewart et al. 1996). The rheological results in AN-105 are of considerable interest to this project because the waste is similar to AN-104 in physical and chemical composition (see Hedengren et al. 2000). Thus we also used AN-105 waste data to confirm the effect of waste disturbance on yield strength. Repeated measurements were taken in risers 16B and 1B. As with AN-104, lithostatic loading may be the cause of increased yield strength with depth. The yield stresses were recomputed from the data taken in 1996. Those passes with similar data were combined. The time between passes is again approximately 50 minutes.

The yield stress as a function of elevation above tank bottom (solids layer depth in AN-105 is approximately 450 cm) is shown in Figures 3.4 and 3.5 for risers 16B and 1B, respectively. As it was in AN-104, the yield stress in the solids layer is reduced by more than a factor of 2 by the repeated disturbance and appears to approach a minimum limit of approximately 40 Pa asymptotically. Figure 3.6 shows the vertical distribution of the yield strength based on the final passes of the ball rheometer at risers 16B and 1B in Tanks AN-104 and AN-105. As indicated in this figure, the yield strength of disturbed AN-104 and AN-105 wastes increases from 5 Pa near the saltcake surface to 62 Pa just above the tank bottoms. Again, the repeated disturbances of the ball rheometer may not represent the effect that mobilization by mixing may achieve.

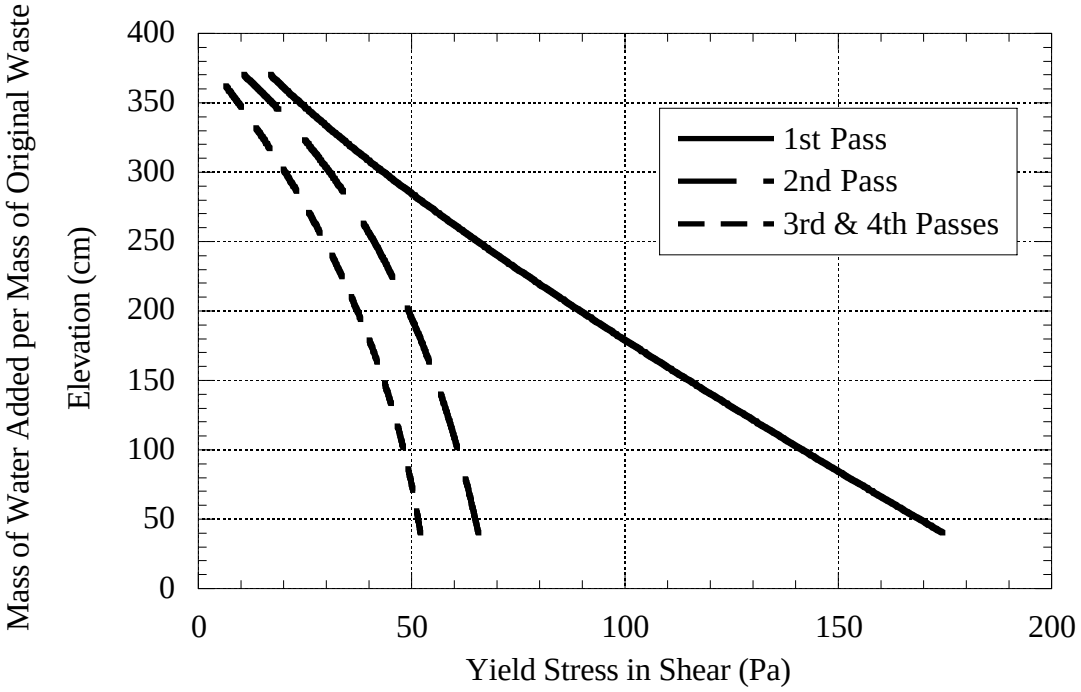

Figure 3.4. Yield Stress in AN-105 from Ball Rheometer, Riser 16B

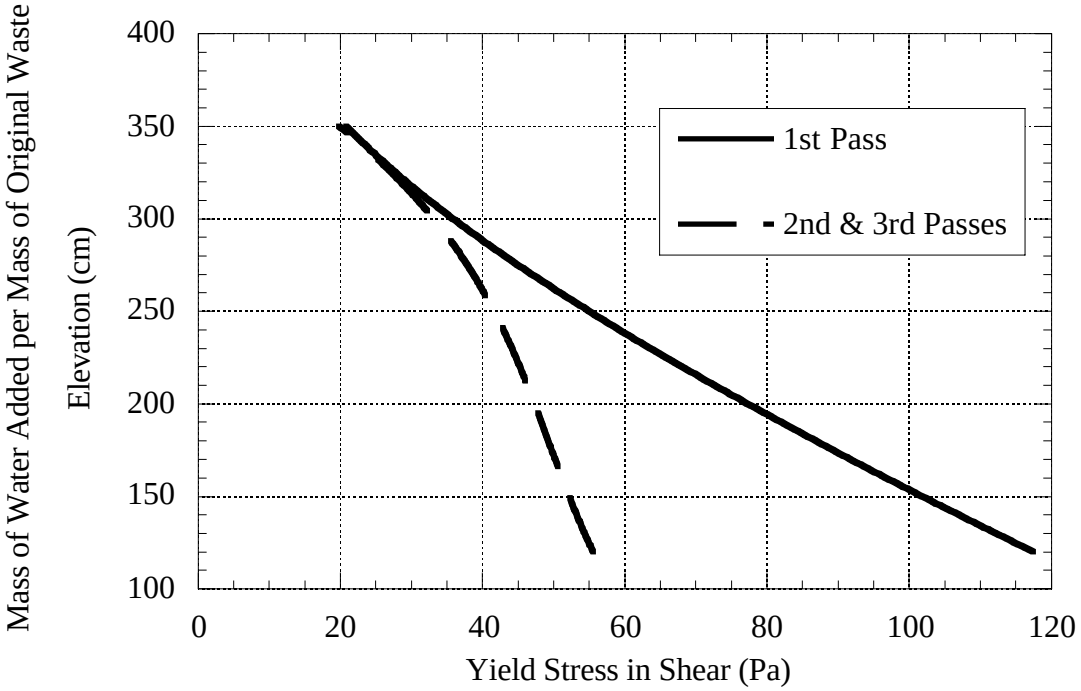

Figure 3.5. Yield Stress in AN-105 from Ball Rheometer, Riser 1B

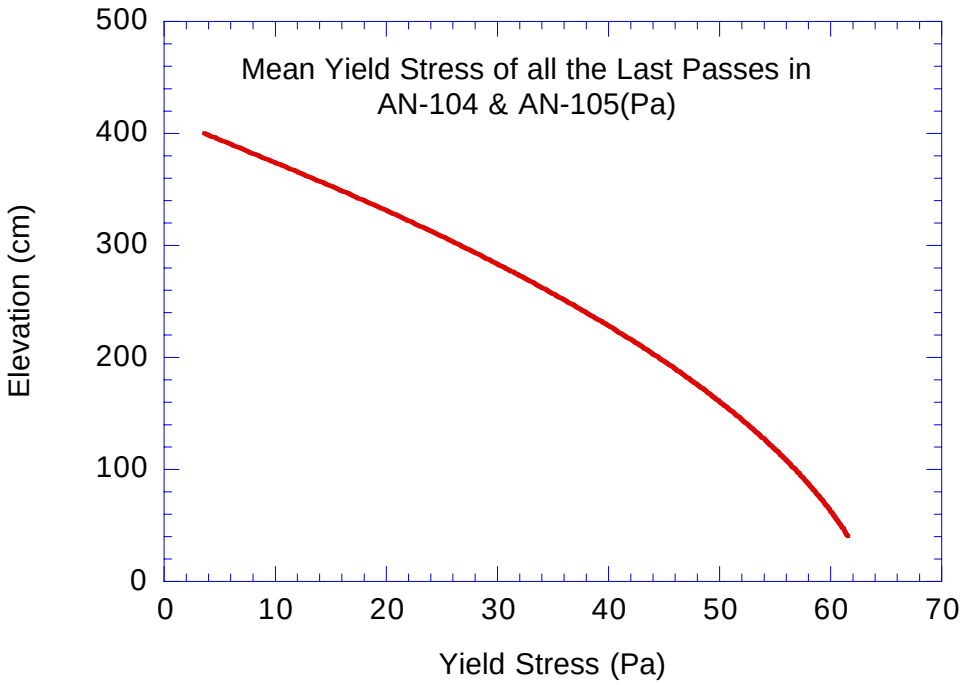

Figure 3.6. In Situ Yield Stress of AN-104 and AN-105 Wastes on Final Passes of the Ball Rheometer

The rheological measurements taken in the laboratory on settled solids samples from AN-105 showed results similar to those from AN-104 (Herting 1997). The disturbance of the sample (prepared like that of AN-104) was sufficient that no yield stress was identified for any case.

3.3.1.3 SY-101 and SY-103 Yield Stress with Disturbance

SY-101 gained notoriety for its large spontaneous releases of flammable gas from the solids layer. The installation of a mixer pump to mix the solids layer and release gas periodically (the mixer pump was operated three times a week) rectified this problem but resulted in excessive growth of a gas-retaining crust and subsequent waste level rise (Johnson et al. 2000). The remediation of these issues required extensive analysis of the tank waste.

The ball rheometer was deployed in SY-101 after the mixer pump was installed, so we have no in situ measurements of the original, undisturbed solids layer. Meyer et al. (1997) extrapolated ball rheometer data from SY-103 to SY-101 conditions that gave an average yield stress in the SY-101 solids layer of approximately 225 Pa.

The average yield stress in shear in SY-103 as determined from the in situ ball rheometer data is approximately 112 Pa (Meyer et al. 1997). The rheological properties of SY-103 waste were also measured experimentally.[(a)] It was noted that:

(a) Bredt PR, JD Hudson, and JM Tingey. 1995. *Effects of Dilution on the Physical, Rheological and Chemical Properties of Tank 241-SY-103 Waste*. Letter Report PNL MIT 092995, Pacific Northwest National Laboratory, Richland, WA.

> Since this property is dependent upon sample history, shear strength had to be measured before the samples experienced high shear rates.

The average laboratory-measured yield stress in shear of the relatively undisturbed samples of the solids layer in SY-103 was approximately 1,500 Pa, significantly higher than the in situ measurement. The suspected cause of this higher reading is the applicability of the viscometer to the waste (varied particle size in a cone-and-plate viscometer, lack of accuracy of the instrument at low strain rates, etc.). Additionally, use of a yield power law to determine the yield point often produces elevated results. The accuracy of this measurement in representing in-tank conditions aside, the importance of the experimental results is observed in the subsequent yield stress measurements after the samples have been mixed into a solids layer composite and stirred. The yield stress values taken two months later in this mixed composite are on the order of 5 Pa. The disturbance significantly reduced the measured yield stress of the solids layer material.

A core sample segment from the well-mixed slurry layer in SY-101 [clearly a convective region without a yield strength; see Meyer et al. (1997) for example] had to be stirred with a spatula for the material to be transferred into a viscometer, demonstrating that ex-tank samples may acquire elevated yield stress values over in situ conditions. This phenomenon is most likely temperature-driven, resulting in the precipitation of solids from the saturated liquid. Upon stirring, however, the material was sufficiently weakened that it could be introduced into the viscometer. No definitive yield stress in shear in the stirred material was subsequently identified.[(a)]

Low shear strengths were observed in other SY-101 samples that had been disturbed. Tingey et al. (1994) stated that:

> Previous experience demonstrates that homogenization [*mixing*] of waste from Tank 241-SY-101 induces a significant decrease in the shear strength of the sample. This decrease was irreversible over a two-year time period

Further, the substantial alteration of the rheological properties of the waste are attributed to processes that induce shear forces, such as homogenization and mixing, which modify the structural configuration of the material. Ignoring, as above, the applicability of the yield stress measurements to in-tank conditions, decreases of an order of magnitude were recorded from the relatively undisturbed samples to those well mixed.

The operation of the mixer pump in SY-101 may also be examined for the effect that mixing has on the yield stress in the solids layer. Full-scale testing of the SY-101 mixer pump began in early 1994. Seven pump operations with the jet pointed at the thermocouple tree in riser 17B [approximately 30 ft (9.1 m) from the pump centerline] were required to mobilize the waste to within 4 in. (0.1 m) of the tank bottom. At riser 17C (32.5 ft [9.9 m] from pump centerline), waste was mobilized down to within 16 in. (0.41) of the bottom after six pump operations. Numerous additional runs were required to mobilize to within 4 in. (0.1 m). This solids material

(a) Correspondence from JF O'Rourke to BE Wells, May 3, 1999. *Results of Viscosity Measurements of Tank 241-SY-101 Samples*. Letter #82100-99-017, Numatec Hanford Corporation, Richland, WA.

had lain undisturbed for months or years (Brewster et al. 1995; Alleman et al. 1994; Stewart et al. 1994). Mixer pump operations were subsequently performed from March 1994 through April 2000 on a schedule of three times per week, with rotations of 30° between each operation offset by 15° after each 180° rotation. As such, the waste at risers 17B and 17C was disturbed approximately once a month. Clearing times to 4 in. (0.1 m) off the tank bottom were typically less than 5 minutes after initiation of pump operation. These observations support that the yield stress of the original solids was much greater than that of the solids disturbed monthly. Some of the significance of these results is lost, however, when it is noted that the original solids was approximately 230 m (5.8 m) thick, while the settled layer during regular mixer pump operations was approximately 50 in. (1.3 m) thick. This was caused not only by the removal of the gas volume but also by the bulk of the fine solids remaining suspended in the supernatant liquid, resulting in an altered make-up of the solids.

The data and evidence from SY-101 and SY-103 indicate that a mixing-type disturbance of the solids layer will significantly reduce the yield stress of the waste material. Further, it is reported that the original yield stress is not regained even after two years.

3.3.1.4 AZ-102 Yield Stress with Disturbance

AN-104 waste is a saltcake whose solids layer consists mainly of soluble solids such as $Na_2CO_3 \cdot H_2O$, $NaNO_3$, Na_2SO_4, and NaF. When these solids are dissolved by the water added to the AN-104 waste through inline and in-tank dilution processes, the remaining solid wastes may appear more like sludge, such as Tank AZ-102 waste. AZ-102 waste is mostly aging waste (neutralized current acid waste) from the PUREX Plant and wastewater. Laboratory measurements of AZ-102 sludge showed yield strength of 1,540 Pa; within a few centimeters of the tank bottom, yield strength is 2,650 Pa.[(a)] Once the sludge was disturbed, the yield strength was reduced to 60 Pa,[(a)] a 26- to 44-fold reduction. When the sludge was mixed with 1.5 times its volume of supernatant liquid, yield strength was reduced to 2 Pa,[(b)] a 700- to 1300-fold reduction from the undiluted, undisturbed sludge. These data indicate that even if the expected AN-101 waste might behave like a sludge waste, the disturbed waste would likely have yield strength of less than 60 Pa.

3.3.2 Effect of Dilution on the Yield Stress in Shear of Solids Layers

Experimental data exist from which the effect on yield stress of diluting a solids layer may be inferred. Typically, to perform dilution analyses on waste samples, water is added to the sample, which is then vigorously mixed. As discussed, the mixing process itself is expected to significantly reduce the yield stress of the material. We therefore examine the data to determine whether dilution increases yield stress of the material by altering its chemical composition.

(a) Gray WJ, ME Peterson, RD Scheele, and JM Tingey. 1993. *Characterization of the First Core Sample of Neutralized Current Acid Waste from Double-Shell Tank AZ-102*. Unpublished report, Pacific Northwest National Laboratory, Richland, WA.

(b) Morrey EV and JM Tingey. 1995. *Comparison of Simulants to Actual Neutralized Current Acid Waste: Process and Product Testing of Three NCAW Core Samples from Tank 101-AZ and 102-AZ*. C95-02-03E, unpublished report, Pacific Northwest National Laboratory, Richland, WA.

No yield stress in shear is identifiable from any of the samples for the dilution studies conducted in AN-104 and AN-105 (Herting 1997, 1998). These particular studies, however, do not truly reflect a newly formed solids layer in a diluted tank because the rheological measurements were taken on recently mixed bulk samples (including the dilution water). In any event, no evidence was shown by these tests of regaining yield stress with dilution that was lost due to disturbance.

The data for the yield stress of the SY-101 solids layer as a function of dilution are affected in a similar fashion. However, Tingey et al. (1995) reported the volume percent of settled solids in the samples, and this may be used to apply some of the lower-dilution tests to our current investigation. The yield stress in shear for samples at 50°C (approximately tank temperature), 70°C, and 90°C as a function of dilution (percent diluent to original waste volume) is shown in Figure 3.7. The volume fraction of settled solids in the sample after dilution is also shown. Note that up to the 25% dilution, it was reported that almost 100% of the sample was still settled solids. There is no evidence that the dilution resulted in a regaining of yield stress and in fact appears to lower it (this lowering may simply be an artifact of the continued disturbance).

Similar data exist for SY-103.[(a)] Figure 3.8 shows the yield stress in shear for the disturbed sample at tank temperature (30°C) as a function of dilution (percent solvent to original waste volume). The volume fraction of settled solids in the sample after dilution is included. Up to 30% dilution, the bulk of the sample was still settled solids. As with the SY-101 data, dilution of the solids appears to lower the yield stress.

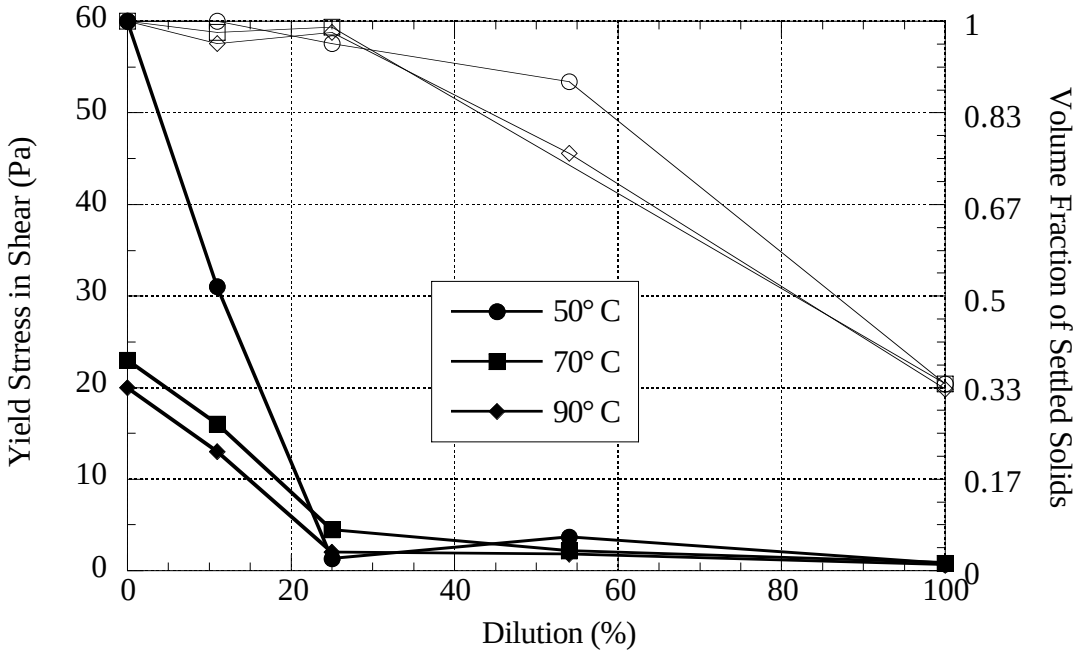

Figure 3.7. Yield Stress in SY-101 Samples

(a) Bredt PR, JD Hudson, and JM Tingey. 1995. *Effects of Dilution on the Physical, Rheological and Chemical Properties of Tank 241-SY-103 Waste*. Letter Report PNL-MIT 092995, Pacific Northwest National Laboratory, Richland, WA.

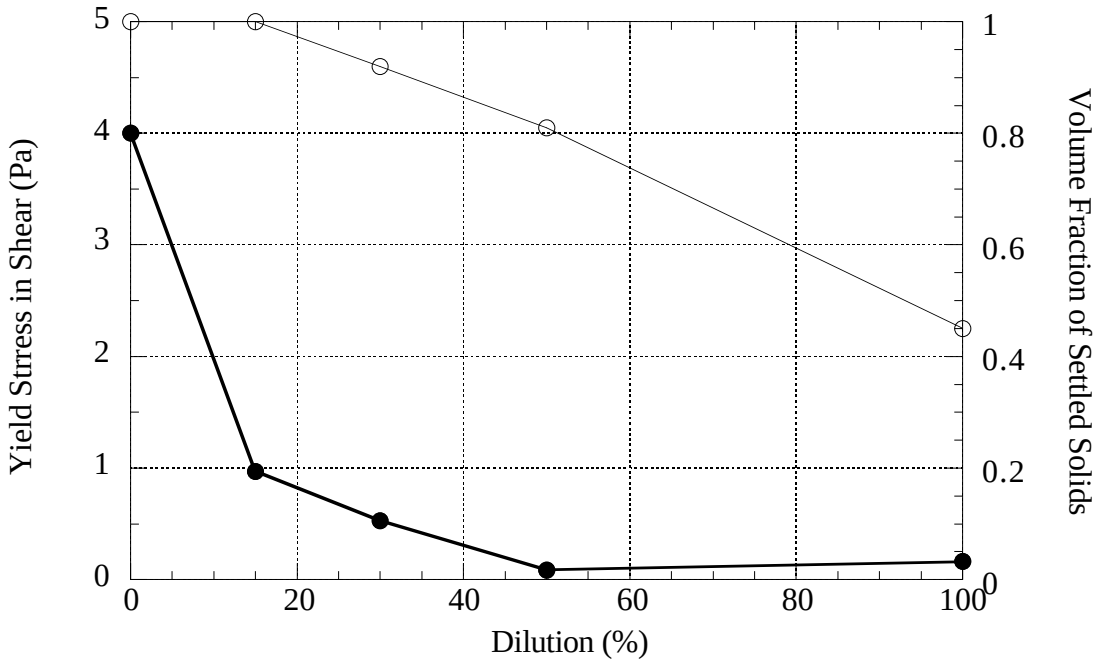

Figure 3.8. Yield Stress in SY-103 Sample at 30°C

No experimental dilution data investigated provided any evidence that dilution would potentially increase the yield stress in shear of the solids. However, all the dilution data taken are for disturbed samples. It is therefore of interest to examine the solids or settled solids chemistry of the diluted waste and to compare this with existing tank waste with rheological measurements. This may provide insight into what the yield stress in the new AN-101 solids layer could potentially become if it is allowed to remain quiescent for extended periods of time.

3.3.3 Solids Waste Chemistry and Yield Stress in Shear of Solids Layers

The predicted AN-101 solids layer chemistry is compared with that of other wastes with measured yield stress in shear. Insight may be provided into what the yield stress in the new solids layer could become if it is allowed to remain quiescent for extended periods of time.

Hanford tank farm physical and chemical data may be accessed through the TWINS database (http://twins.pnl.gov). Examination of this database identified a number of Hanford tanks with measured yield stress in shear. Tanks in which the ball rheometer was deployed were also considered. Those tanks, along with their solids chemistry (presented as mass of solid species per total mass of solids), yield stress in shear, and data sources are listed in Table 3.2. The entries for yield stress with three values indicate the median, maximum, and minimum of the reported measurements. The predicted waste chemistry of the AN-101 solids layer (see Section 2) is included for comparison. No definitive match in chemical composition is apparent. A possible trend is that a higher proportion of insoluble solids potentially results in greater yield stress.

3.3.4 Yield Stress in Shear Summary

No conclusive data exist to define the yield stress in shear of the predicted solids layer in AN-101. Examination of the available data supports the understanding that the disturbance and dilution the material will undergo prior to settling as a new solids layer will significantly reduce the yield stress below its current levels in AN-104.

The most definitive data are from the ball rheometer measurements taken in situ, which indicate that the average yield stress of the AN-104 solids layer reduces to 50 Pa or less when disturbed. It is expected that the disturbance of the solids will actually be much greater than that caused by the ball rheometer, and the data support that the yield stress would therefore be even further reduced. Additionally, the reduced depth of the AN-101 solids layer decreases the lithostatic loading. Thus, the maximum yield strength may be less than that of the original AN-104 waste. The data also support that dilution of the solids will further reduce the yield stress. From the chemical composition, there may be evidence that the yield stress may be increased due to the diluted state of the waste. There is no evidence, however, that the yield stress of the material will be regained within the time frame expected prior to pretransfer mobilization of the new solids layer in AN-101.

The yield strength of AN-101 waste would be less than the original, undisturbed, undiluted, in situ yield strength of 150–170 Pa measured in AN-104, and most likely less than 60 Pa, unless the AN-101 waste would be undisturbed over a period of years. Thus, we conducted a series of AN-101 pump jet mixing simulations with yield strength varying from 1, 5, 20, 60, 100, and 150 Pa as a parametric evaluation.

3.3.5 Volume of Solids Transferred from AN-104 to AN-101 by Supernatant Decant Process

There are two mechanisms by which AN-104 solids may be transferred to AN-101. The first mechanism results from a spontaneous gas release that would mobilize the solids during the AN-104 supernatant liquid transfer to AN-101. The second is slurry transfer after the AN-104 saltcake has been diluted and mixed. For the first process, under a separate project, Pacific Northwest National Laboratory developed a supernatant liquid decant model to evaluate waste retrieval strategies. Tank AN-104 was included. Using the AN-104 decant model, we conducted a Monte Carlo simulation to determine the amount of solids that would be transferred during the AN-104 supernatant liquid transfer to Tank AN-101.

Decanting supernatant liquid out of AN-104 will most likely cause buoyant displacement gas release events (BDGREs), as presented in Wells et al. (2002). A BDGRE occurs when a portion, or "gob," of the solids layer accumulates sufficient gas to become buoyant with respect to the overlying liquid. The gob then breaks free of the surrounding solids and rises to the surface, where it releases a portion of its gas into the tank headspace. The gob is assumed to sink back to the solids layer after releasing enough gas to become negatively buoyant. It is expected that these BDGREs triggered during the decant will release approximately 12% of the gas retained in the solids layer and will suspend a portion of the solids layer in the supernate.

Table 3.2. Waste Solids Chemistry and Yield Stress

Tank	Solids Phase											Yield stress (Pa)
	Mass of Solids Phase per Total Solids Mass											
	Data source											Data source
AN-101 (Predicted)	$Ca(OH)_2$	$Cr(OH)_3$	$Na_2C_2O_4$	Na_3PO_4 $12H_2O$	SiO_2							
	0.02	0.15	0.42	0.37	0.05							
	Predicted (see Section 2)											
AN-103	$Ca(OH)_2$	$Na_2C_2O_4$	Na_2CO_3	Na_2SO_4	Na_3PO_4	Na_4SiO_4	$NaAlO_2$	$NaNO_3$				142 ±15
	0.01	0.04	0.14	0.01	0.01	0.01	0.37	0.41				Meyer et al. (1997)
	Calculated from Lambert (1998a)											
AN-104	$Cr(OH)_3$	$Na_2C_2O_4$	Na_2CO_3 H_2O	Na_2SO_4	Na_3PO_4 $12H_2O$	NaF	$NaNO_3$	SiO_2				81 ±11
	0.03	0.13	0.31	0.18	0.12	0.02	0.19	0.01				Meyer et al. (1997)
	Calculated from TWINS											
AN-105	Cr_2O_3	$Na_2C_2O_4$	Na_2CO_3	Na_2SO_4								129 ±31
	0.01	0.14	0.69	0.13								Meyer et al. (1997)
	Herting (1997)											
SY-101 (pre-1999)	$Na_2C_2O_4$	Na_2CO_3	$NaAl(OH)_4$	$NaNO_2$	$NaNO_3$	Insol.						225 ±100
	0.14	0.28	0.11	0.10	0.26	0.11						Meyer et al. (1997)
	Hudson et al. (1995)											
SY-103	Cr_2O_3	Fe_2O_3	$Na_2C_2O_4$	Na_2CO_3	Na_2SO_4	Na_3PO_4	$NaAl(OH)_4$	NaCl	NaF	$NaNO_2$	$NaNO_3$	112 ±40
	0.05	0.03	0.10	0.25	0.04	0.08	0.29	0.01	0.01	0.08	0.07	Meyer et al. (1997)
	Calculated from Lambert (1998b)											
AZ-101	$Al(OH)_3$	$Ca(OH)_2$	$Fe(OH)_3$	$Na_2C_2O_4$	Na_2CO_3 H_2O	Na_2SO_4	NaF	$NaNO_2$	$NaNO_3$	SiO_2		1,770 (4,190-235)
	0.27	0.01	0.27	0.03	0.01	0.20	0.05	0.08	0.07	0.02		TWINS
	Calculated from TWINS data											
AZ-102	$Al(OH)_3$	$Cr(OH)_3$	Na_2SO_4	NaF	SiO_2							866 (12,100-345)
	0.87	0.02	0.05	0.01	0.05							TWINS
	Onishi et al. (2000)											
AY-101	$Al(OH)_3$	$Ca_5(OH)(PO_4)_3$	Cr_2O_3	FeOOH	$LaPO_4$ $2H_2O$	MnO_2	$Na_2C_2O_4$	$NaAlSiO_4$	$Ni(OH)_2$	$Pb(OH)_2$		2,020 (18,300-45)
	0.43	0.02	0.01	0.36	0.01	0.01	0.13	0.01	0.01	0.01		TWINS
	Preliminary Environmental Simulation Program (ESP) results[(a)]											
AY-102	$Al(OH)_3$	$Ca_5(OH)(PO_4)_3$	Cr_2O_3	FeOOH	$LaPO_4$ $2H_2O$	MnO_2	$Na_2C_2O_4$	$Na_2U_2O_7$	$Ni(OH)_2$	$Pb(OH)_2$		507 (8,100-57)
	0.33	0.04	0.01	050	0.01	0.04	0.03	0.01	0.01	0.01		TWINS
	Preliminary Environmental Simulation Program (ESP) results[(a)]											

Table 3.2. Waste Solids Chemistry and Yield Stress

Tank	Solids Phase											Yield stress (Pa)
	Mass of Solids Phase per Total Solids Mass											
	Data source											Data source
AW-101	$Na_2C_2O_4$	Na_2CO_3	Na_2SO_4	Na_3PO_4	NaF							159 ±37
	0.20	0.59	0.07	0.11	0.08							Meyer et al. (1997)
	Herting (1999)											
AW-103	$Al(OH)_3$	$KAlSiO_4$	$Na_2C_2O_4$	$Na_2U_2O_7$	NaF	ZrO_2						587 (3,540-279)
	0.15	0.02	0.01	0.03	0.41	0.37						TWINS
	Preliminary Environmental Simulation Program (ESP) results[(a)]											
B-111	Bi_2O_3	$Ca_5(OH)(PO_4)_3$	CrOOH	FeOOH	$Na_2C_2O_4$	$NaAlCO_3(OH)_2$	$NaFPO_4$ $19H_2O$	$Pb(OH)_2$				90
	0.20	0.02	0.01	0.25	0.05	0.03	0.42	0.02				TWINS
	Preliminary Environmental Simulation Program (ESP) results[(a)]											
B-201	Bi_2O_3	CaF_2	Cr_2O_3	FeOOH	$KAlSiO_4$	$LaPO_4$ $2H_2O$	MnO_2	$Na_2C_2O_4$	$SrCO_3$			1,265 (1,310-1,220)
	0.52	0.06	0.02	0.09	0.03	0.13	0.12	0.01	0.01			TWINS
	Preliminary Environmental Simulation Program (ESP) results[(a)]											
C-104	$Al(OH)_3$	$Ca_5(OH)(PO_4)_3$	FeOOH	$MnOH_2$	$Na_2C_2O_4$	$Na_2U_2O_7$	$NaAlSiO_4$	NaF	$NiOH_2$	ZrO_2		848 (7,080-289)
	0.37	0.01	0.08	0.02	0.07	0.08	0.09	0.12	0.01	0.15		TWINS
	Preliminary Environmental Simulation Program (ESP) results[(a)]											
C-107	$Al(OH)_3$	Bi_2O_3	FeOOH	MnO_2	$Na_2U_2O_7$	$NaAlSiO_4$	$NaFPO_4$ $19H_2O$	$NiOH_2$	$Pb(OH)_2$			1,050 (7,830-75)
	0.34	0.02	0.34	0.01	0.02	0.02	0.21	0.01	0.02			TWINS
	Preliminary Environmental Simulation Program (ESP) results[(a)]											
T-107	$Al(OH)_3$	Bi_2O_3	CaF_2	FeOOH	$Na_2U_2O_7$	$Na_4P_2O_7$ $10H_2O$	$NaAlCO_3(OH)_2$	$NaAlSiO_4$	NaF	$NaFPO_4$ $19H_2O$		720
	0.22	0.03	0.01	0.13	0.08	0.33	0.04	0.07	0.04	0.03		TWINS
	Preliminary Environmental Simulation Program (ESP) results[(a)]											
U-107	$Al(OH)_3$	Cr_2O_3	FeOOH	$Na_2C_2O_4$	$NaFPO_4$ $19H_2O$	$NaNO_3$	NaPHOH $12H_2O$					130 (550-30)
	0.10	0.01	0.01	0.01	0.03	0.62	0.23					Hedengren et al. (2001)
	Preliminary Environmental Simulation Program (ESP) results[(a)]											

(a) Personal Communication with LA Mahoney, June 28, 2002.

We evaluated the amount of suspended solids and how much is transported out of the tank. The decant model and analysis methods as excerpted/paraphrased from Wells et al. (2002) are summarized below, and the solids volume transfer results are presented. The decant model simulates the behavior of a number of gobs of gas-bearing solids during the decant process. It is intended for use in tanks that currently exhibit BDGREs.

The data and observations pertaining to BDGREs indicate that the solids layer in those tanks experiencing BDGREs consists of a collection of on the order of 10 to 15 discrete regions, or gobs, in different stages of gas retention (Meyer et al. 1997; Meyer and Stewart 2001). In-tank video during large gas releases in SY-101 show clearly a series of local upwellings from different areas of the tank. Waste temperature profiles before and after BDGREs observed in other DSTs show the effects of very few of them, indicating localized events. Additionally, based on actual gas release volumes, solids layer depth, and gas volumes required for buoyancy, only a portion of the solids layer has produced BDGREs. Finally, this gob concept describes the observed BDGRE period in relation to the gas generation rate for the BDGRE tanks.

Similar behavior is assumed to occur during decant. The initial conditions are determined by tank historical behavior and measured data, as is the actual gas release behavior when a BDGRE occurs during decant. However, because it is not equivalent to accelerated "natural" gas generation, gas expansion and buoyancy during decant are calculated with a detailed model that simulates the process. The cumulative effect of gas generation on the retained gas volume over the several days required for decant is negligible and is ignored. However, the minimal background contribution to the headspace hydrogen concentration is included.

The mechanism that triggers gas release during decant is decreasing supernate depth. This reduces hydrostatic pressure on the gas stored in the solids and causes it to expand, increasing the gas volume fraction. Stored gas was assumed to expand isothermally as an ideal gas. Gobs with sufficient initial retained gas volume will become buoyant and undergo BDGREs. The gas growth and buoyancy calculation accounts for nonuniform vertical profiles of pressure and gas fraction as indicated by in-tank measurements (Hedengren et al. 2000). The gas fraction required for release is slightly greater than for neutral buoyancy to account for the restraining effect of the surrounding non-buoyant solids.

The gas release volume is determined by the gob's initial conditions and the condition of the supernatant layer at the time it becomes buoyant. Obviously, the largest gobs with the highest initial gas fraction release the most gas. However, the fraction of the gas released decreases with hydrostatic pressure, so earlier releases tend to be larger. A gob releases gas because some of the potential energy released during its rise to the surface yields the material that has trapped gas bubbles. The potential energy available decreases with supernate depth and will eventually become insufficient to yield the rising material. Gobs that become buoyant after that point are assumed not to release gas.

When a BDGRE occurs, gas is assumed to be released from the gob at the same time-varying rate as during spontaneous BDGREs. The resulting headspace hydrogen concentration is the result of superposition of all gobs that have been released, those still completing a release, and the background gas generation of the remaining waste (supernate and solids). The headspace

atmosphere is assumed to be fully mixed. Besides ventilation flow, the calculation accounts for increasing headspace volume due to decant and gas release from the solids. Ventilation outflow is assumed fixed, and the inflow includes the effects of decant pumping and gas release rates.

The gas release process is assumed to result from a fraction of the gob volume disintegrating to allow bubbles to escape. A fraction of the portion of the gob that disintegrates in this process is assumed to become mixed in the supernate and not resettle with the rest of the spent gob. The fractional rate of mixing is assumed to be the same as fractional gas release rate. Material thus mixing in the supernate is assumed to remain there for the duration of the decant. Suspension of the heavier solid particles increases the supernatant density and reduces the neutral buoyancy gas fraction for gobs that have not previously become buoyant. This may make additional gobs buoyant immediately and allow subsequent gobs to become buoyant earlier than they would have without mixing. The dominant effect is to allow multiple BDGREs to be triggered by the first one. The supernatant depth above gobs that have not become buoyant is reduced to account for volume reductions resulting from gas release and resuspension during earlier BDGREs.

The majority of the physical waste parameters required for the modeling described above have significant, quantified uncertainties. A deterministic calculation with all parameters set to bounding values has no physical or statistical meaning. Instead, we must account for all the parameter uncertainties and establish the overall probability distribution for the model's predictions. To accomplish this, a large number of model simulations need to be run with input parameter sets selected from their respective distributions. The collection of output values from all the model simulations then forms the desired overall probability distribution.

A Monte Carlo simulation approach was used here. This approach can determine the uncertainty of modeling results when the input parameters have uncertainty distributions. For each retrieval operation modeled, 5,000 simulation runs were conducted. Simulating a large number of cases allows all important physical effects included in the model to influence the predicted behavior. The result is a set of model outputs, each with its own set of predicted results, that constitutes a probability distribution over those predicted results. This allows us to predict the probability of a given result given the input probability distributions.

The suspension of solids, as discussed above, obviously allows for the transfer of those solids during the supernatant decant. We generated solids transfer volume output distributions with a Monte Carlo simulation of the decant model. The results are summarized in Table 3.3. The

Table 3.3. Solids Transferred from AN-104 by Supernatant Decanting

Result (units)	Median	95% CL
Vtotal (m^3)	6.6	26.3
FS	0.03	0.10
HS (in)	4.0	15.8
MF	0.005	0.020
AF	0.003	0.012
MD (kg/m^3)	1,446	1,513
AD (kg/m^3)	1,444	1,510

output distributions are presented in Figures 3.9 through 3.15. Input parameter distributions are identical to those used in Wells et al. (2002). The results in Table 3.3 include the following:

1. Total dry solids volume removed from AN-104 (assumes solids density of 2,300 kg/m^3) (Vtotal)
2. Fraction of dry solids in the solids layer in AN-104 transferred out (FS)
3. Height of solids layer transferred out (degassed height; no in-line dissolution/etc. accounted for) (HS)
4. Maximum solids volume fraction during transfer (MF)
5. Average solids volume fraction during transfer (AF)
6. Maximum slurry density during transfer (no dilution included) (MD)
7. Average slurry density during transfer (no dilution included) (AD).

At the 95% confidence limit (CL), 10% of the solids in the solids layer are transferred out of AN-104 by supernatant decanting, and the maximum solids volume fraction in the transfer line at the 95% CL is 2%.

In Figures 3.9 through 3.15, the histogram serves as a visual explanation for the shape of data. Each bar shows the frequency of occurrence of the value or range of values represented on the abscissa, which is separated into intervals. Through observation of a histogram plot, one may quickly ascertain the general shape as normal (Gaussian), skewed, uniform, bimodal, etc. Accompanying the histogram is an outlier box plot. The outlier box plot is a schematic that allows one to see the sample distribution and identify points with extreme values, or outliers, that cannot be so easily seen on the histogram due to small numbers of points at the tails. The ends of the box are the 25th and 75th quantiles, also called the quartiles. The difference between these two quartiles is called the interquartile range. The line across the middle identifies the median. The ends of the whiskers are the outer-most data points from their respective quartiles that fall within the distance computed as 1.5 times the interquartile range. Thus, both plots together (the histogram and the outlier box plot) provide a more complete picture of the distribution. The bracket along the edge of the box identifies the shortest half of the distribution, which is the densest 50% of the observations.

The model results (see Table 3.3) indicate that 233 ft^3 (6.6 m^3) of dry solids (or 2.5 vol% of the original AN-104 solids) as the median value would be transferred to AN-101 during the supernatant liquid transfer. This results in a 4-in. (0.1 m) solids layer in AN-101. The 95% confidence limits of the dry solids volume and solids layer thickness are 929 ft^3 (26.3 m^3) (10 vol% of the original solids) and 15.8 in. (0.40 m), respectively. However, the inline and in-tank dilution water would eventually dissolve much of these transferred solids, as discussed in Section 2.

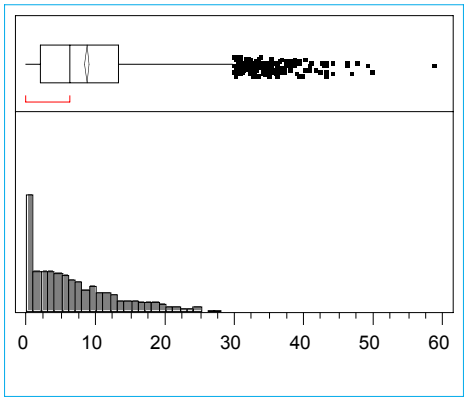

Figure 3.9. Total Dry Solids Volume Removed from AN-104 - Vtotal (m^3)

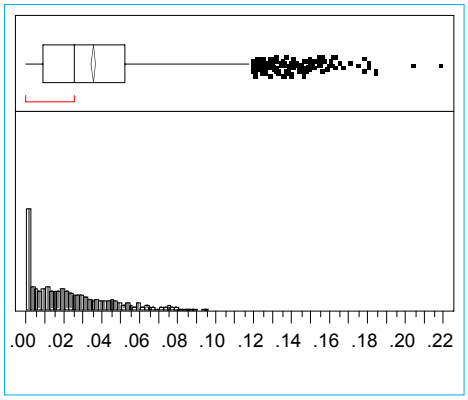

Figure 3.10. Fraction of Dry Solids in the Solids Layer in AN-104 Transferred Out - FS

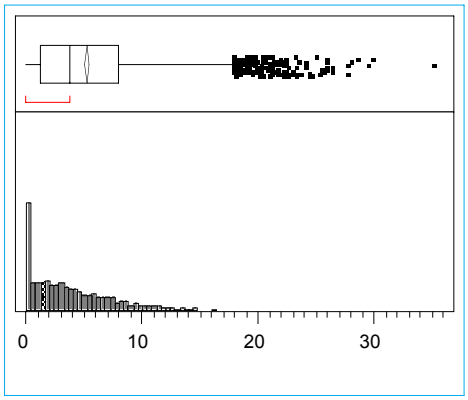

Figure 3.11. Height of Solids Layer Transferred Out - HS (in.)

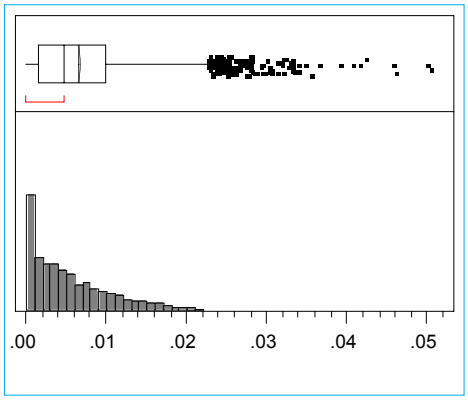

Figure 3.12. Maximum Solids Volume Fraction During Transfer - MF

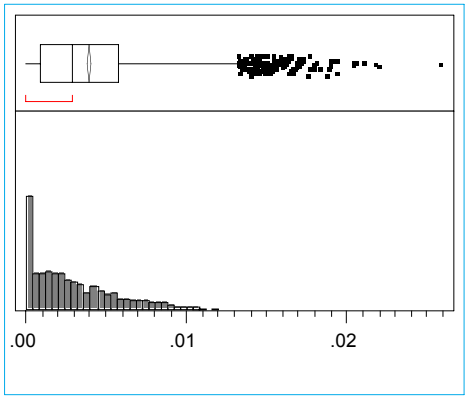

Figure 3.13. Average Solids Volume Fraction During Transfer - AF

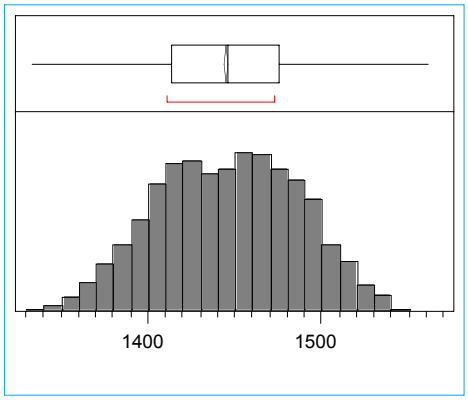

Figure 3.14. Maximum Slurry Density During Transfer - MD (kg/m^3)

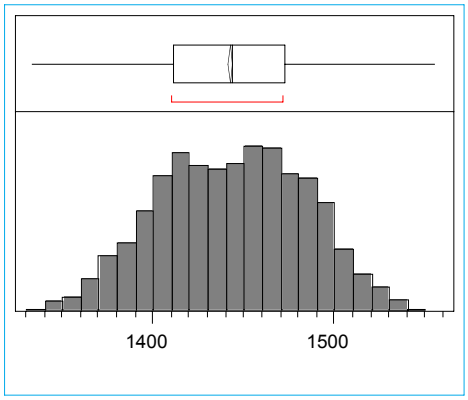

Figure 3.15. Average Slurry Density During Transfer - AD (kg/m^3)

4.0 Pump Jet Mixing Simulation Results

4.1 Simulation Conditions

The expected AN-101 waste would be multicomponent and multiphase, consisting of solids and liquid, as discussed in Sections 2 and 3. The current waste retrieval plan calls for using two mixer pumps located 20 ft (6.1 m) from the tank center to mix the waste in AN-101. In this section, we describe the AN-101 pump jet mixing simulation with the three-dimensional code, TEMPEST (Onishi and Trent 1999) to determine whether a single rotating 300-hp mixer pump that is 20 ft (6.1 m) from the tank center could adequately mix the expected AN-101 tank waste (see Figure 4.1).

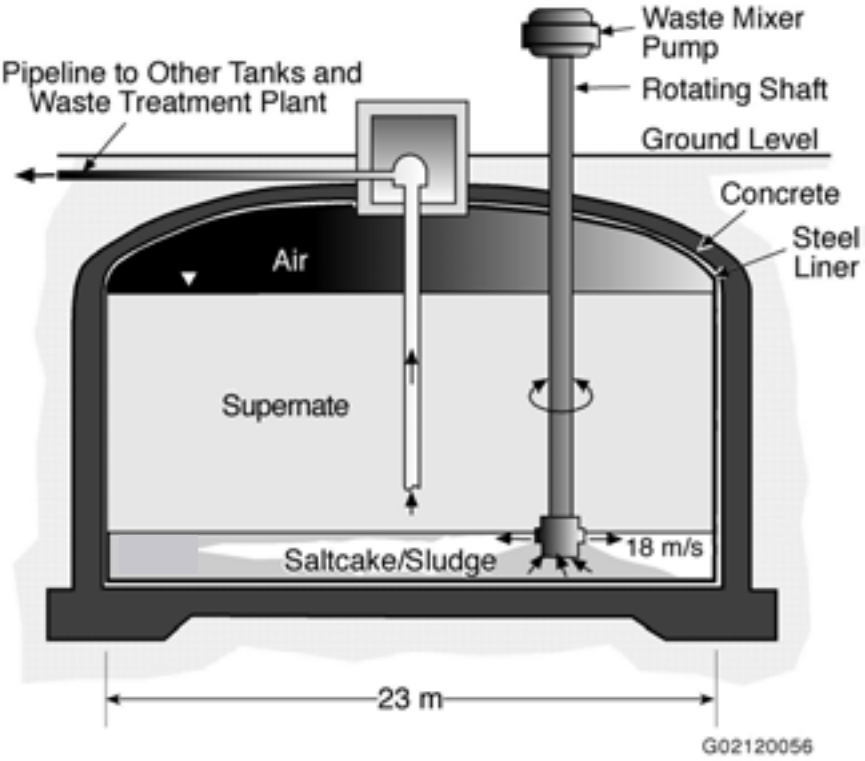

Figure 4.1. Waste Mixing with a Single Off-Center Pump

The mixer pump with rotating injection nozzles mixes the solids and liquid in the tank. The baseline pump is a 300-hp, centrifugal pump with a 17-in.- (0.43-m-) diameter intake at the bottom and two 6-in.- (0.15-m-) diameter nozzles injecting 60-ft/sec (18.3-m/s) jets 11 in. (0.28 m) above the pump intake (see Figures 4.1 and 4.2). An alternative pump, called here as an inverted pump is shown in Figure 4.3. It has two 6-in.- (0.15-m-) diameter injection nozzles at the pump bottom and a 27-in. (0.67-m-) diameter intake 21.5 in. (0.55 m) above the injection nozzle centerlines. This pump configuration can potentially enhance solids erosion by placing injection nozzles closer to the tank bottom and eases pump startup by having the inlet higher (Onishi et al. 2002).

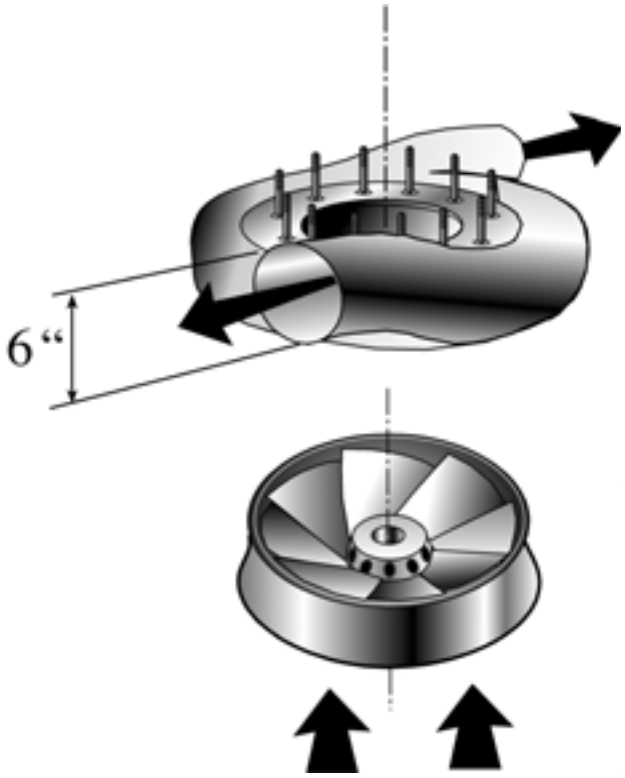

Figure 4.2. Baseline Pump with Intake Below Injection Nozzles
(lower part of figure shows pump impellers)

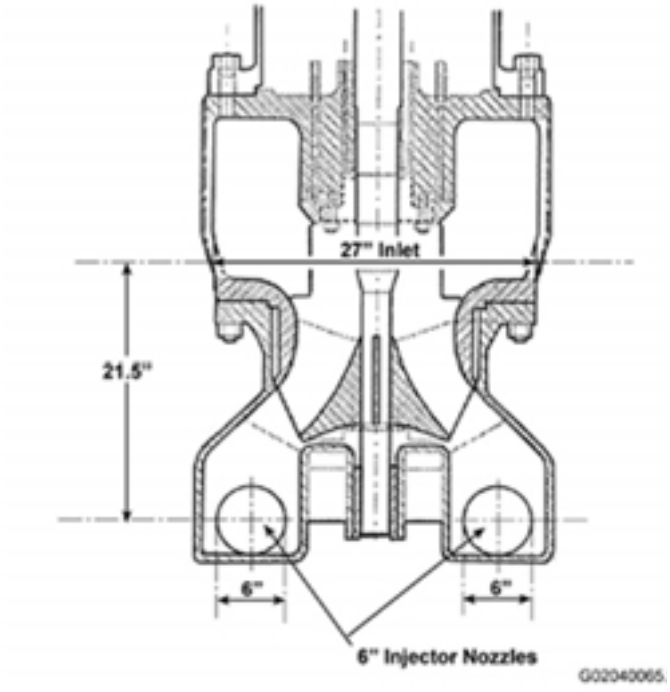

Figure 4.3. Example of Inverted Pump with Injection Nozzles Below Pump Intake

To mobilize the waste, the mixer pumps must overcome yield strength and high viscosity and mix the solids with the overlying liquid waste. As discussed in Section 3, AN-101 waste is expected to have a yield strength less than150 Pa and most likely less than 60 Pa due to waste disturbance and dilution. We selected yield strengths of 1, 5, 20, 60, 100, and 150 Pa as a parametric evaluation and potential bounding value for the AN-101 pump jet mixing simulations. The waste volume and properties are also presented in Section 3. The nine modeling cases shown in Table 4.1 were evaluated in this study.

Table 4.1. Modeling Cases Evaluated in this Study

Simulation Cases	Pump Type	Yield Strength, Pa
Case 1	Baseline pump with intake below the injection nozzles	1
Case 2		5
Case 3		20
Case 4		60
Case 5		100
Case 6		150
Case 7	Inverted pump with injection nozzles below the pump inlet	60
Case 8		100
Case 9		150

4.2 Baseline Mixer Pump with Intake Below Injection Nozzles

As discussed in Sectrion 3.1, we divided the AN-101 solids into four particle size fractions, as shown in Table 3.1. Predicted erosion and solid distribution patterns were the same for all four solids. Solid 3 results are presented here. The initial condition of the AN-101 model is shown in Figure 4.4. The top plot is along the 3 o'clock vertical plane (Vertical r-z plane, I = 2), and the bottom plot is along the 9 o'clock vertical plane (vertical r-z plane, I = 21). Each of the two rotating jets is shown in the two plots. The mixer jets along vertical plane 2 would travel the shortest distance (17.5 ft or 5.33 m) to reach the tank wall, while the jets along vertical plane 21 must travel the longest distance (57.5 ft or 17.5 m) to reach the tank wall.

Figure 4.4 shows the initial 18.9-in.- (0.48-m-) thick solids layer at the bottom and 266.1-in.- (6.76-m-) thick liquid layer, totaling 285.0-in. (7.238-m) of waste and water in AN-101. It also shows the position of the rotating pump, its withdrawal inlet 7 in. (0.18 m) above the tank bottom, and a 6-in. (0.15-m) nozzle 18 in. (0.46 m) above tank bottom, which would inject a 60-ft/sec (18.3-m/s) jet near the surface of the solids layer. The solid line indicates the tank boundary. The presence of the velocity vector indicates that the area is within the tank.

The lower plot of Figure 4.4 shows the time (0 simulation second) and the solids concentration as volume fraction (volume fraction of 1 being 100 vol%). The right side of the lower plot of the figure, for example, describes which vertical plane it is showing (in the lower plot it is an r-z plane, which is Vertical Plane 21 (I = 21) oriented at the 9 o'clock position, and an area of plot coverage on these vertical planes (in this case J = 1 to 32, indicating the entire

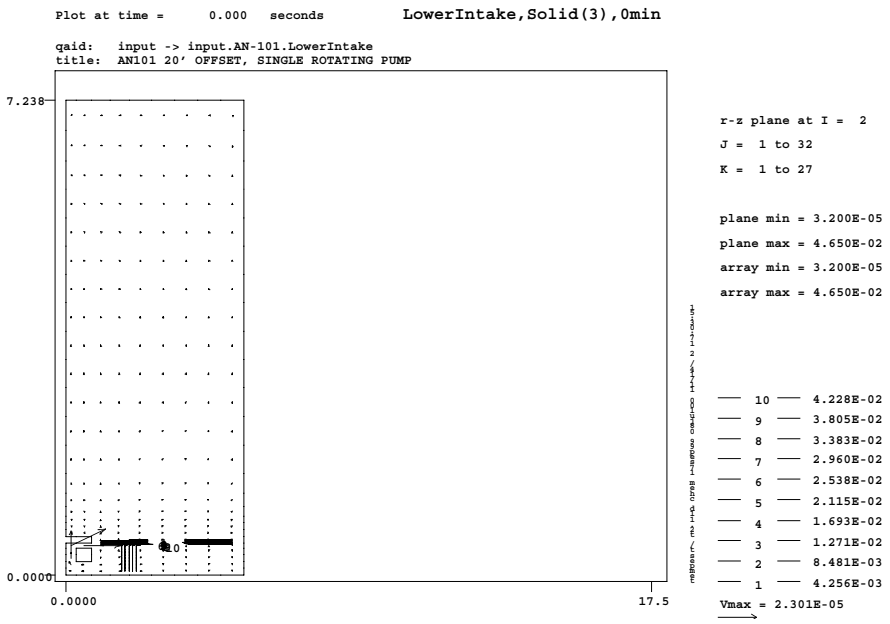

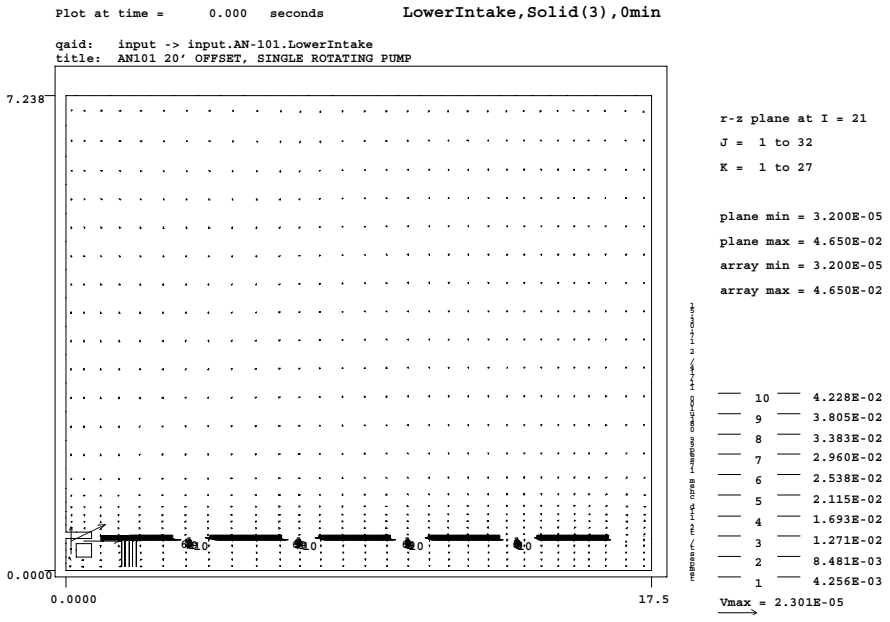

Figure 4.4. Initial AN-101 Waste Condition with Baseline Pump (intake below injection nozzles)

horizontal direction from the pump center to the tank wall 17.5 m away, and K = 1 to 27, indicating the vertical direction from the tank bottom to the waste surface at 7.238 m). The right sides of these plots also show solids concentrations (expressed in volume fractions) represented by Lines 1 through 10. Plane min and max indicate the minimum and maximum values [solids volume fractions of 3.2×10^{-5} (0.0032 vol%) and 0.0465 (4.65 vol%), respectively, in this case] within the plotted planes, while array min and max indicate the minimum and maximum values [solids volume fractions of 3.2×10^{-5} (0.0032 vol%) and 0.0465 (4.65 vol%), respectively, in this case] encountered within the entire tank simulation area. The Solid 3 concentration in the solids layer is 4.65 vol%, as shown in the figure (also see Table 3.1). The initial solids concentration in the liquid layer was assigned a small value (0.0032 vol%) rather than zero to accommodate the settling velocity of the solids for all solids concentrations. As shown, we diluted the solids layer in the immediate vicinity of the mixer pumps as the initial condition to reflect the expected waste condition after installing the mixer pump. Dilution also assists in starting up the mixer pumps.

At the lower right of the plots, the maximum velocity on the vertical plane is shown (in this case 2.301×10^{-5} m/s) with its corresponding scale lengths. All velocities in this figure are scaled to this magnitude. The jet velocity at the nozzle exit was assigned to be 60 ft/sec (18.3 m/s).

Predicted final solids erosion patterns along the jet pass that are the shortest (along Vertical Plane 2) and longest to the tank wall (along Vertical Plane 21) are shown in Figures 4.5 through 4.10 for yield strengths of 1, 5, 20, 60, 100, and 150 Pa, respectively. In each of these six cases, both rotating jets are orienting along the shortest and farthest planes to the tank wall at the specific simulation times shown in the figures. The maximum velocities in the figures represent maximum velocities inside the pump. At the nozzle exit, the jet velocity was 18.3 m/s (60 ft/sec).

These figures indicate that predicted solids even at the farthest tank wall were mobilized by the single baseline mixer pump in all yield strength cases. Model results indicate that the smaller the yield strength, the greater the solids mobilization by the mixer pump. Table 4.2 shows the solids erosion amount and average thickness of the solids layers that are not eroded. The table also presents the predicted pump operation time required to arrive at the final erosion pattern for these six baseline pump cases. The baseline pump would mobilize 78.6 to 100% of the solids, depending on the yield strength. As shown in Table 4.2, the solids in the bottom 3–4-in. (0.07–0.1 m) on average would be left un-eroded for waste with yield strength above 20 Pa.

Table 4.2. Predicted Erosion of AN-101 Solids Layer by a Single Off-Center Baseline Pump

Simulation cases	Yield strength, Pa	Pump operation time, minutes	Solids erosion amount, vol%	Remaining solids layer thickness, in. (m)
Case 1	1	20	100	0
Case 2	5	40	100	0
Case 3	20	40	85.1	2.8 (0.072)
Case 4	60	40	80.1	3.8 (0.096)
Case 5	100	110	79.5	3.9 (0.098)
Case 6	150	120	78.6	4.0 (0.103)

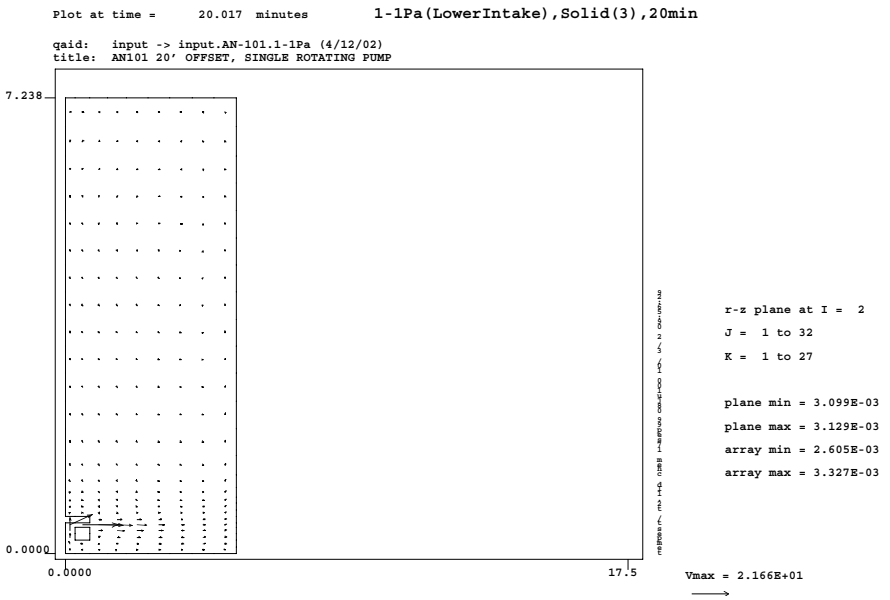

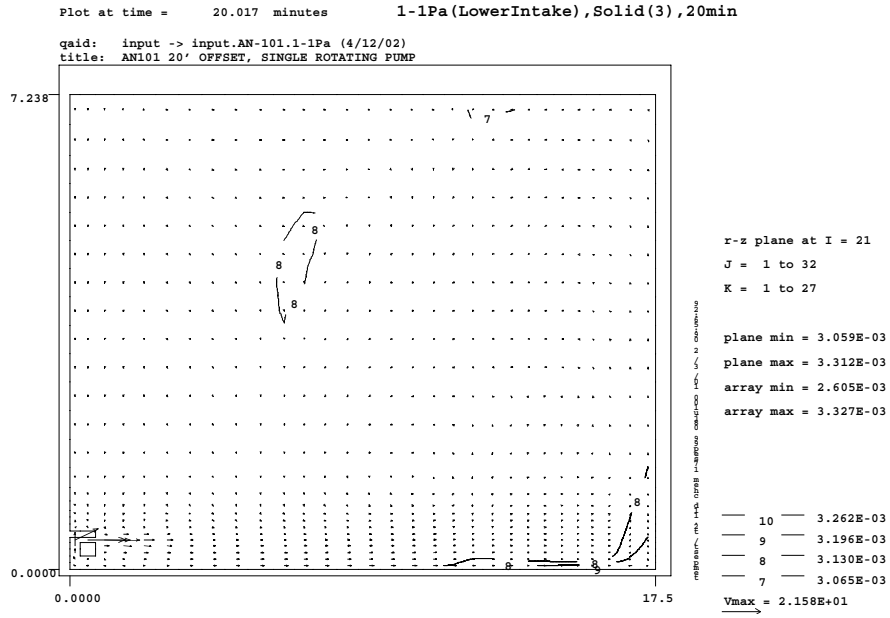

Figure 4.5. Baseline Pump (intake below injection nozzles): Predicted Erosion of AN-101 Solids Layer with 1-Pa Yield Strength at 20 Simulation Minutes

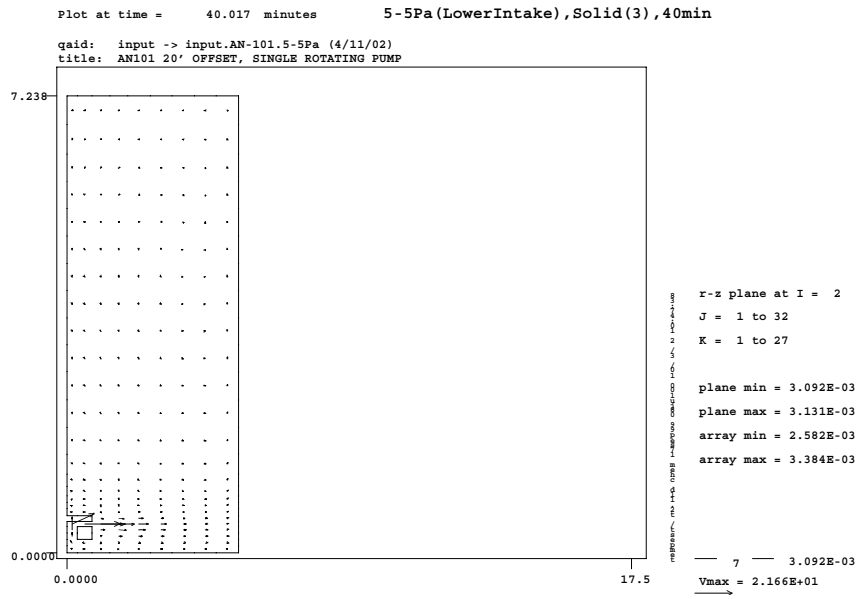

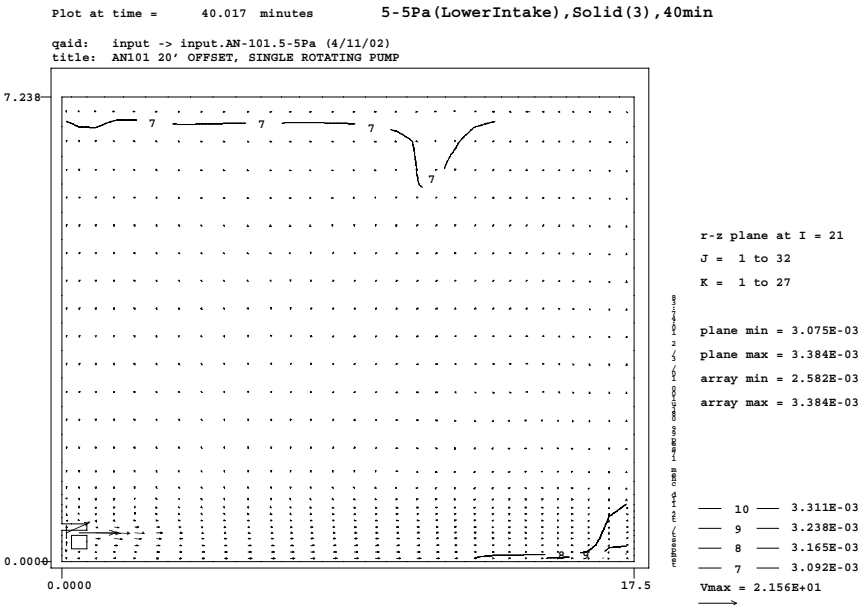

Figure 4.6. Baseline Pump (intake below injection nozzles): Predicted Erosion of AN-101 Solids Layer with 5-Pa Yield Strength at 40 Simulation Minutes

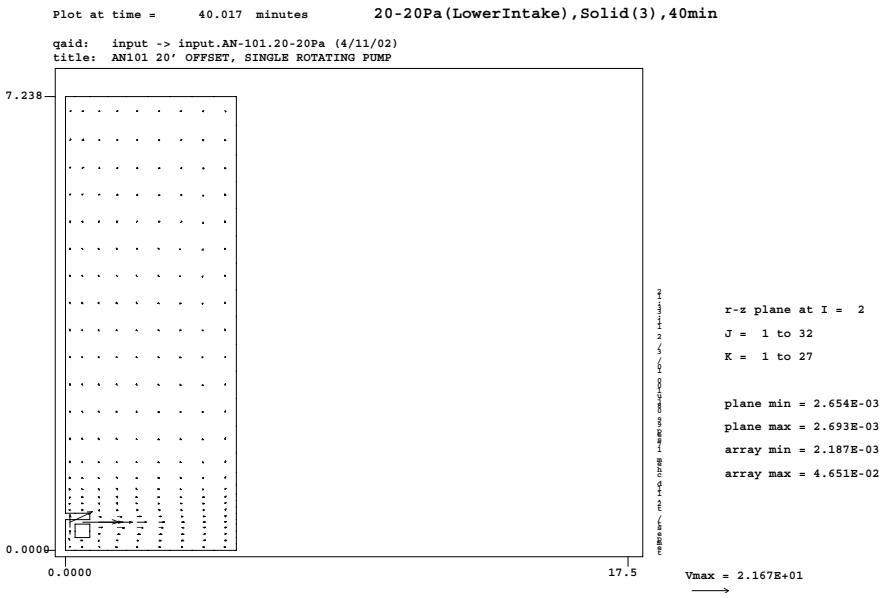

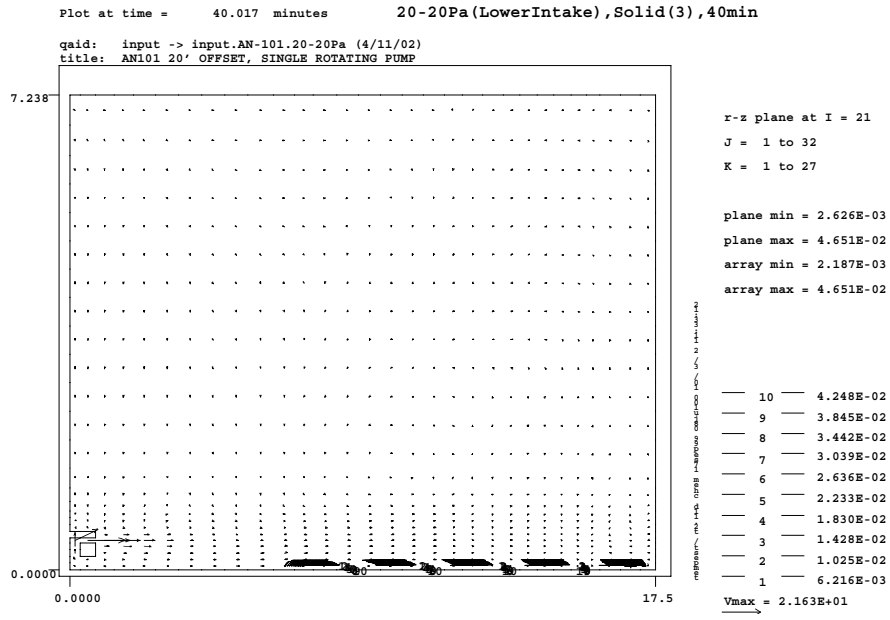

Figure 4.7. Baseline Pump (intake below injection nozzles): Predicted Erosion of AN-101 Solids Layer with 20-Pa Yield Strength at 40 Simulation Minutes

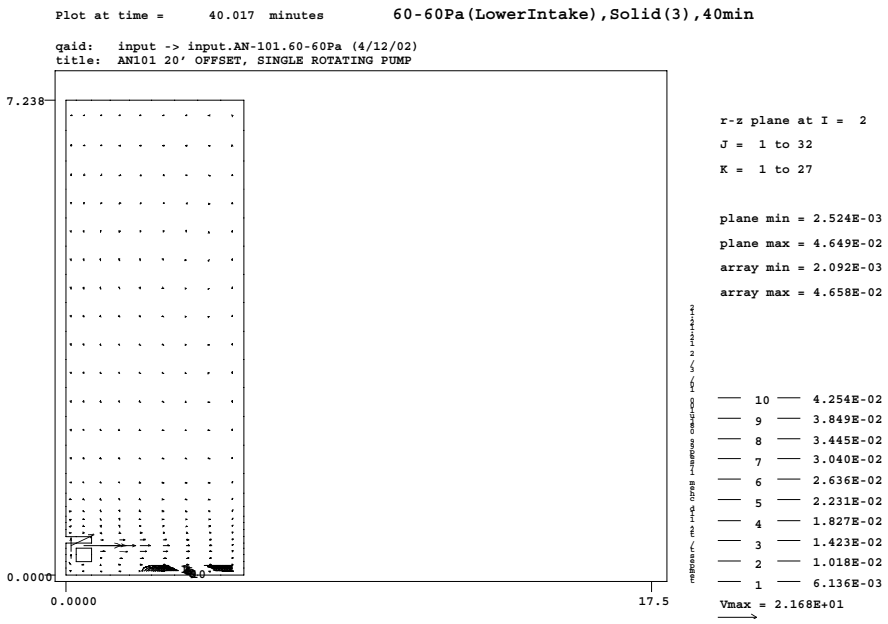

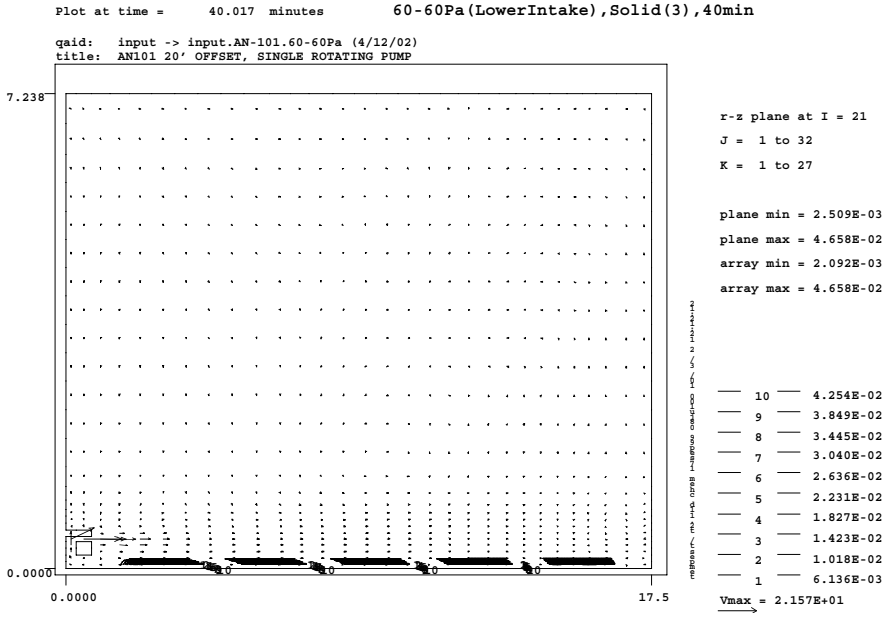

Figure 4.8. Baseline Pump (intake below injection nozzles): Predicted Erosion of AN-101 Solids Layer with 60-Pa Yield Strength at 40 Simulation Minutes

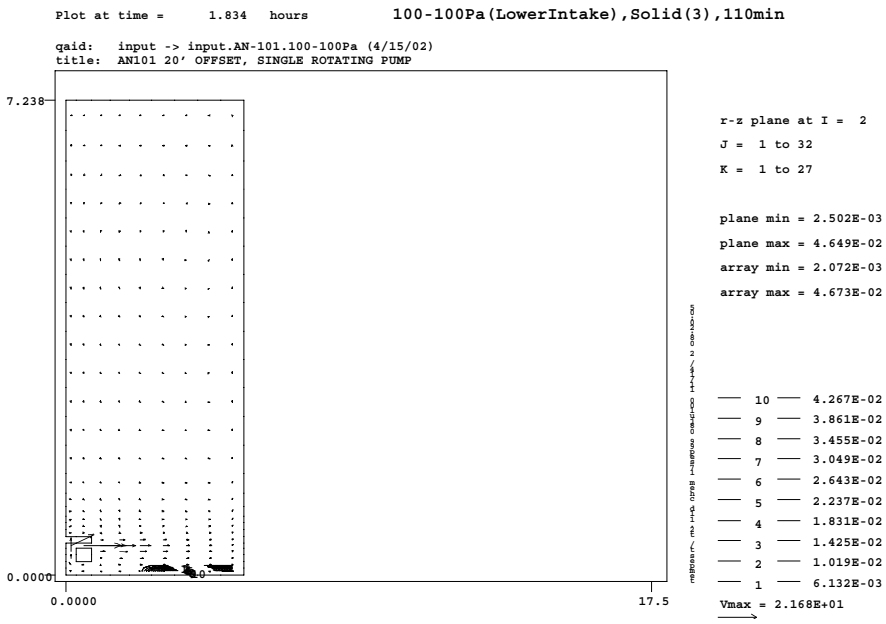

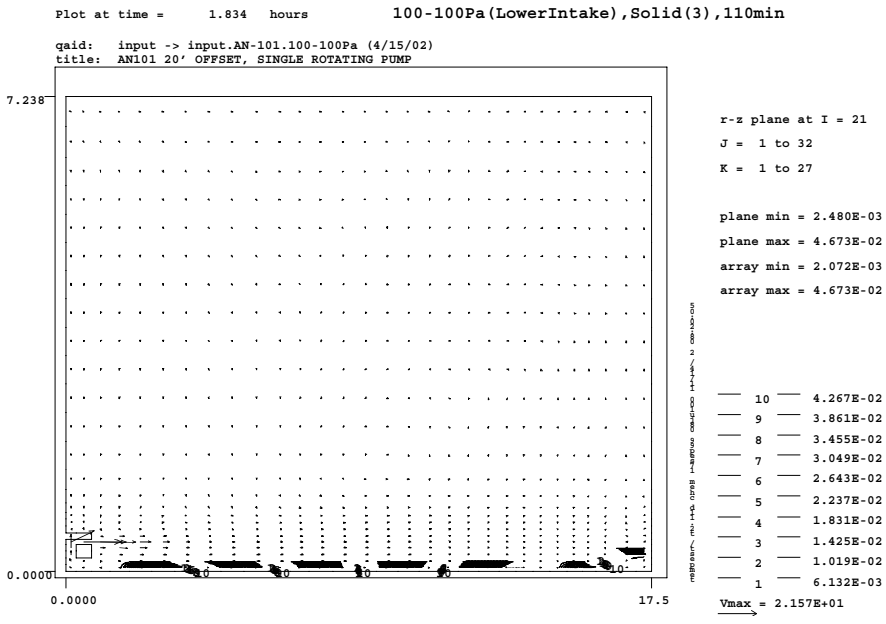

Figure 4.9. Baseline Pump (intake below injection nozzles): Predicted Erosion of AN-101 Solids Layer with 100-Pa Yield Strength at 110 Simulation Minutes

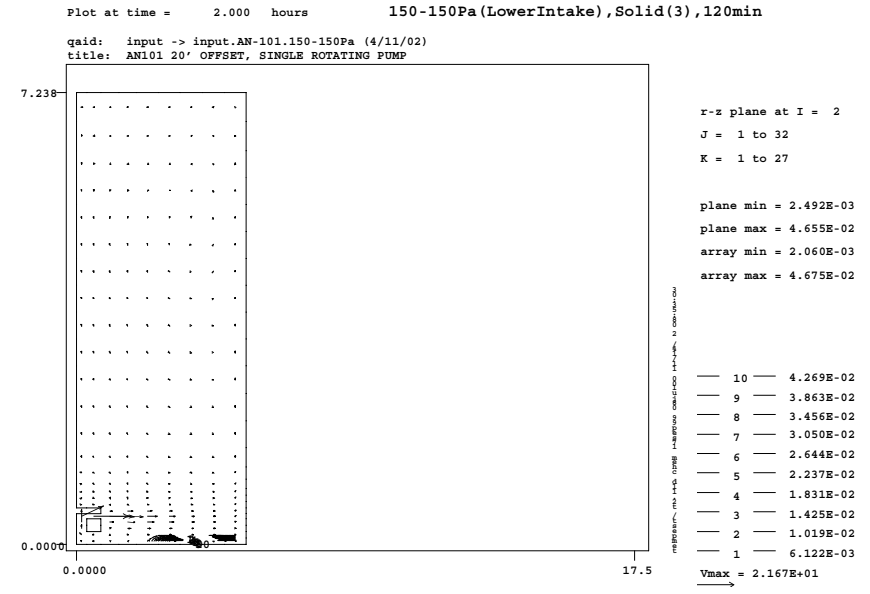

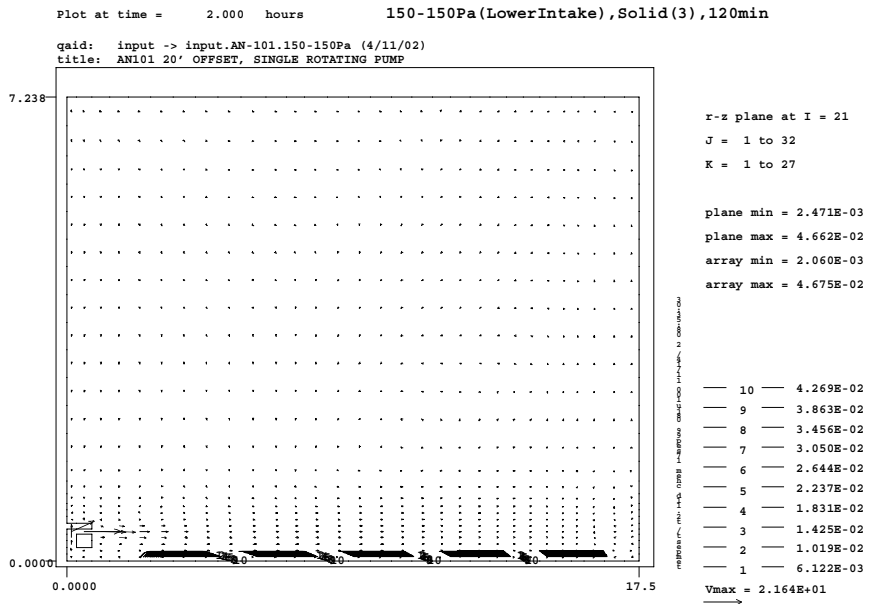

Figure 4.10. Baseline Pump (intake below injection nozzles): Predicted Erosion of AN-101 Solids Layer with 150-Pa Yield Strength at 120 Simulation Minutes

4.3 Single Inverted Mixer Pump with Injection Nozzles Below Inlet

In a previous study, Onishi et al. (2002) reported that the inverted pump with bottom injection would erode more sludge than the baseline pump. In this study, we modeled the inverted pump for yield strengths of 60, 100, and 150 Pa. Initial conditions for the expected AN-101 waste to be mixed with the inverted pump are shown in Figure 4.11 with the bottom injection and top inlet positions.

The predicted solids erosion pattern and velocity distribution for the 60, 100, and 150 Pa cases along the shortest and farthest distances (Vertical Planes 2 and 21) are shown in Figure 4.12 through 4.14. As in the baseline pump cases, these figures indicated that a single 20-ft (6.1-m) off-center, inverted mixer pump would mobilize solids at the farthest tank wall but eroded solids a little closer [average within 2–3 in. (0.05–0.08 m)] to the tank bottom than the baseline pump, which eroded solids to within average of 3–4 in. (0.07–0.1 m) above the tank bottom.

Table 4.3 shows the predicted solids erosion amount and average thickness of the solids layers that are not eroded. The inverted pump would mobilize 83.6 to 89.3% of the AN-101 solids for the cases modeled, with yield strength of 60, 100, and 150 Pa. (For yield strength less than 20 Pa, the inverted pump is expected to mobilize 100% of the solids because it is expected to mobilize at least as much as the baseline pump.) This is slightly more than the baseline pump would erode. The table also presents mixing time required to arrive at the final erosion conditions for these three inverted pump cases, showing shorter mixing time to reach the final erosion condition for the 100 and 150 Pa cases (but not the 60 Pa case) than those of the corresponding baseline pump cases. These simulation results of baseline and inverted pumps indicate that a single off-center pump can mobilize the expected AN-101 solids, even those farthest from the mixer pump.

Table 4.3. Predicted Erosion of AN-101 Solids Layer by Single Off-Center Inverted Pump

Simulation Cases	Yield Strength, Pa	Required Erosion Time, min	Solids Erosion Amount, vol%	Remaining Solids Layer Thickness, in. (m)
Case 7	60	55	89.3	2.0 (0.051)
Case 8	100	75	86.1	2.6 (0.067)
Case 9	150	75	83.6	3.1 (0.079)

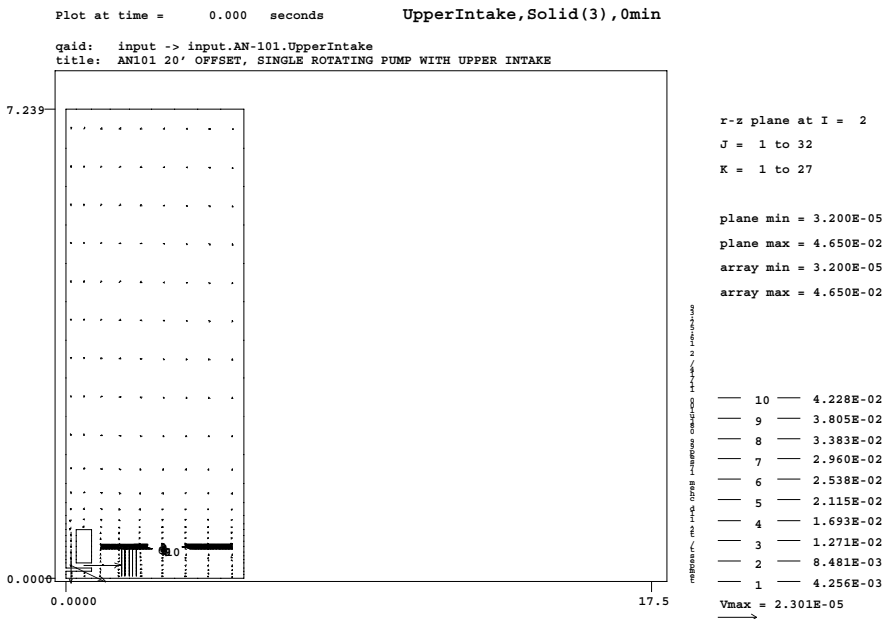

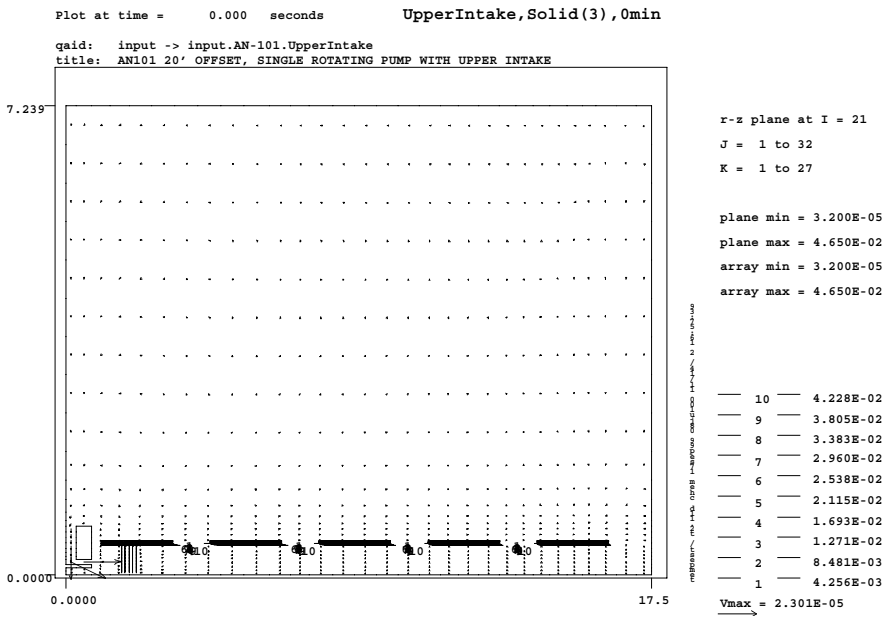

Figure 4.11. Initial AN-101 Waste Condition with Inverted Pump (injection nozzles below pump inlet)

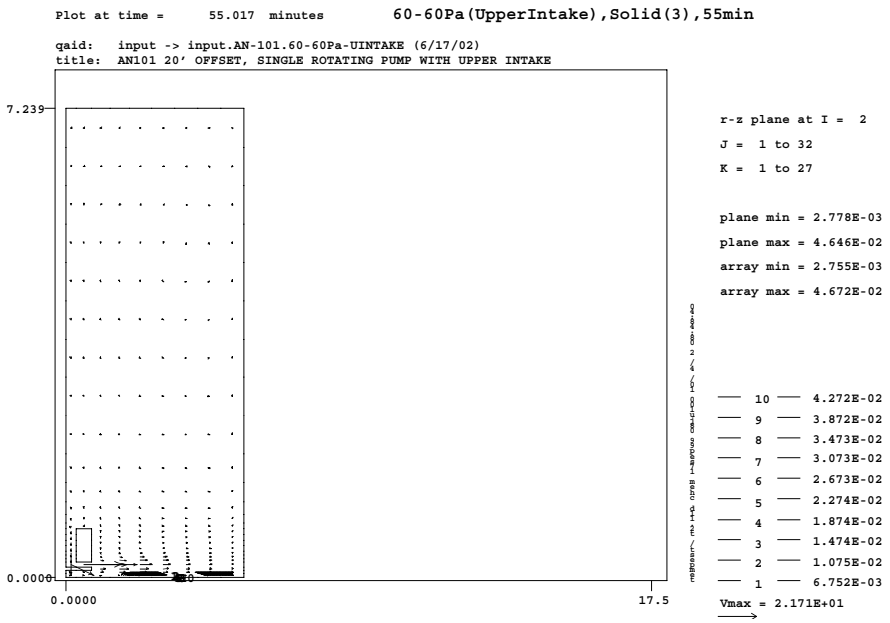

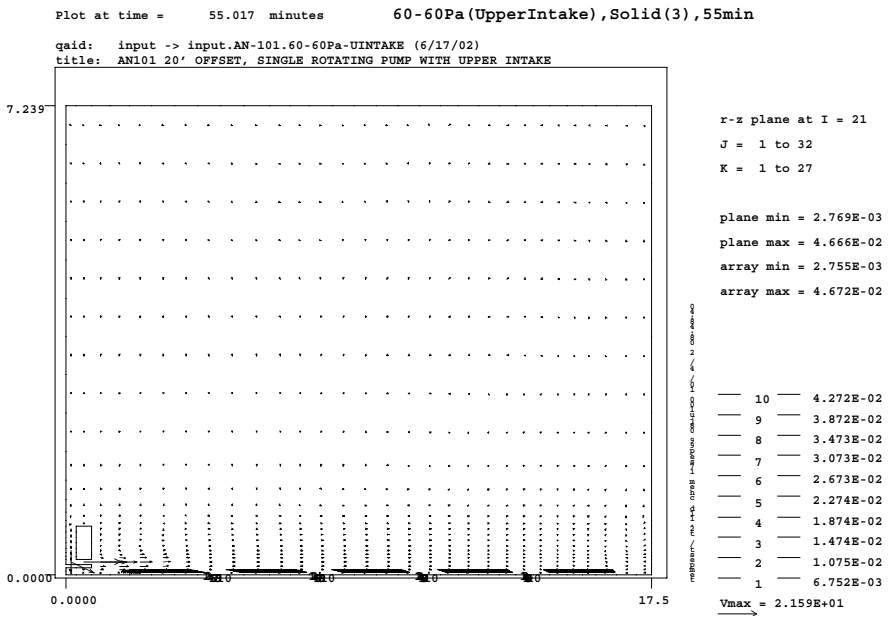

Figure 4.12. Inverted Pump (injection nozzles below pump intake): Predicted Erosion of the AN-101 Solids Layer with 60-Pa Yield Strength at 55 Simulation Minutes

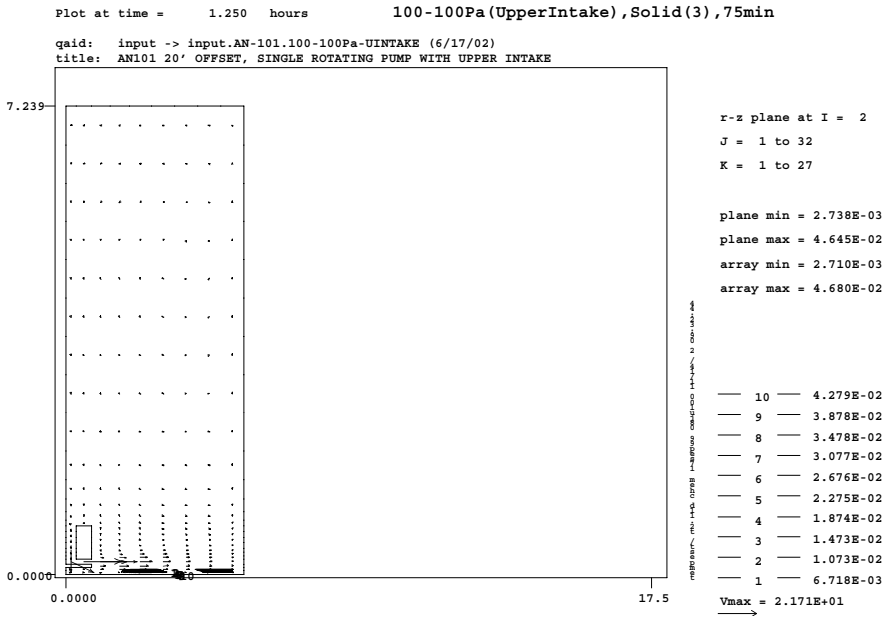

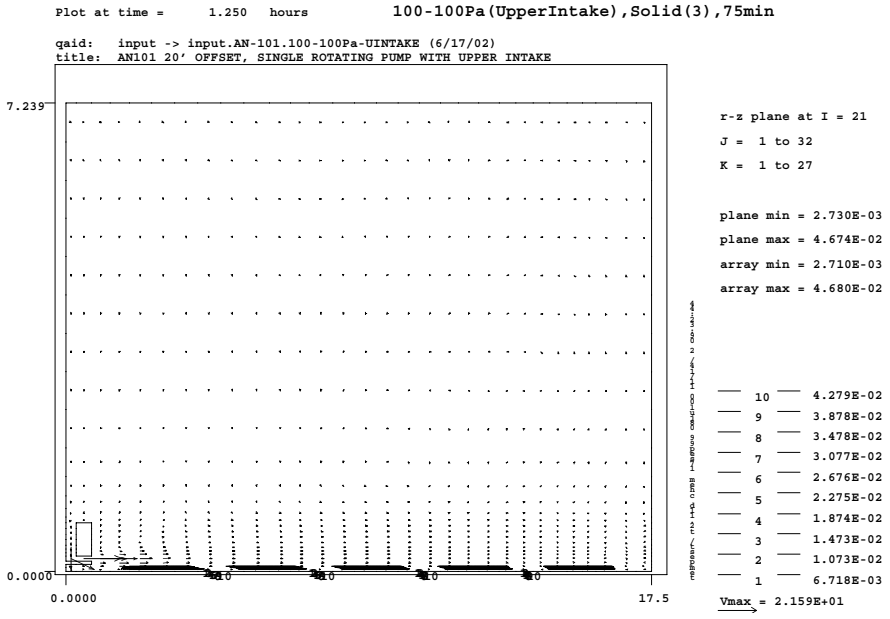

Figure 4.13. Inverted Pump (injection nozzles below pump intake): Predicted Erosion of the AN-101 Solids Layer with 100-Pa Yield Strength at 75 Simulation Minutes

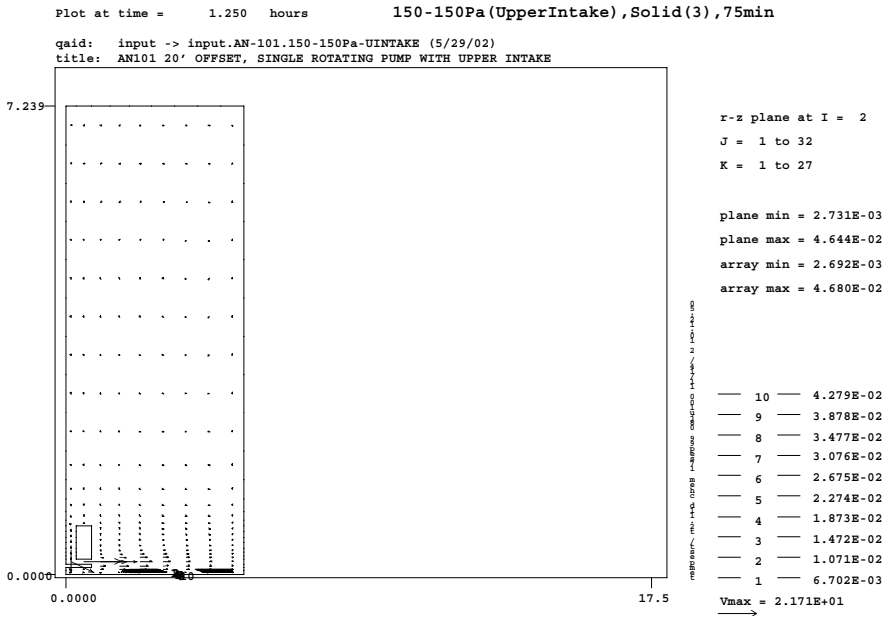

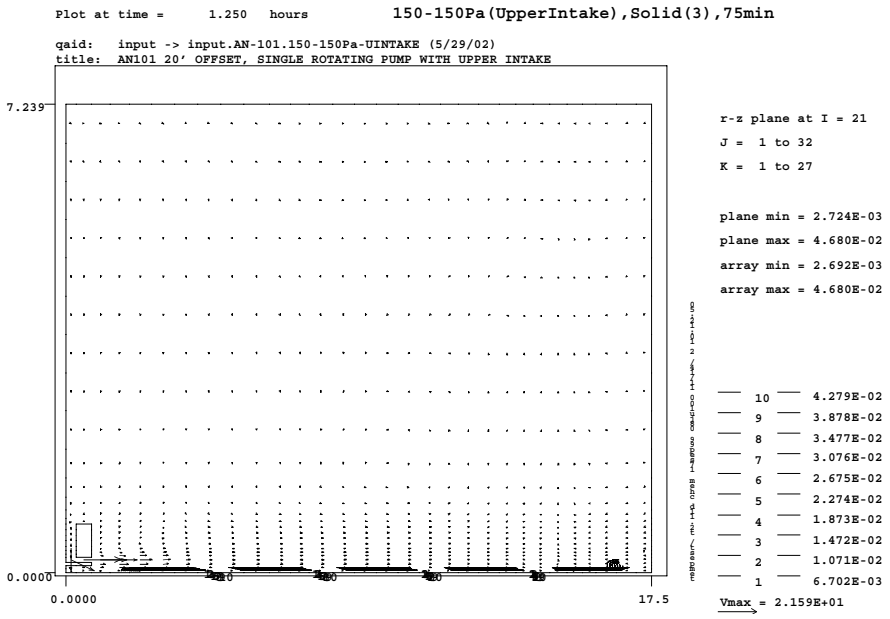

Figure 4.14. Inverted Pump (injection nozzles below pump intake): Predicted Erosion of the AN-101 Solids Layer with 150-Pa Yield Strength at 75 Simulation Minutes

5.0 Summary and Conclusions

The current waste retrieval plan calls for using two mixer pumps located 20 ft (6.1 m) from the tank center to mix waste stored in Hanford Tank AN-101. The objective of this evaluation was to determine whether a single rotating 300-hp mixer pump located at this position could adequately mix the expected AN–101 tank waste. The tank currently contains 12 in. (0.33 m) of supernatant liquid. The current plan projects that the tank would receive inline and in-tank diluted AN-104 waste in the years 2005, 2007, and 2008. The expected AN-101 waste will be a mixture of the following:

- The original 12-in.- (0.33-m-) thick AN-101 liquid waste
- 40% in-line dilution of AN-104 supernatant liquid with water
- 43% in-tank dilution of AN-104 saltcake with water.

Chemical modeling indicates that solids present in AN-104 saltcake are $Na_2CO_3 \cdot H_2O$, $NaNO_3$, $Na_2C_2O_4$, Na_2SO_4, NaF, $Cr(OH)_3$, $Na_3PO_4 \cdot 12H_2O$, SiO_2, and $Ca(OH)_2$, in order of abundance. Mixing of original AN-101 liquid waste and inline and in-tank diluted AN-104 waste with water would dissolve all $Na_2CO_3 \cdot H_2O$, $NaNO_3$, Na_2SO_4, and NaF, of AN-104 solids, resulting in an 88% reduction (in molality) in solid wastes. Thus, the diluted waste stored in AN-101 would be

- 18.9 in. (0.48 m) solids layer
- 266.1 in. (6.76 m) liquid layer
- 285.0 in. (7.24 m) total waste.

To mobilize the waste, the mixer pumps must overcome yield strength and high viscosity, and mix the solids with the overlying liquid waste. The expected AN-101 solids layer would have weak yield strength because of waste disturbance and dissolution through repeated in-tank pump jet mixing, inline and in-tank dilution of AN-104 waste, and pipeline transfer. Because there are no measured rheology data on the expected AN-101 waste, we evaluated the effects of waste disturbance and solids dissolution on yield strength with available data from Tanks AN-104, AN-105, SY–101, SY-103, AZ-102, and many others. Based on these data, we determined that the yield strength of the AN-101 would be less than the original undisturbed AN-104 yield strength of 150 Pa and most likely less than 60 Pa.

Thus, we selected the yield strength to be 1, 5, 20, 60, 100, and 150 Pa for the AN-101 pump jet mixing simulations as a parametric evaluation. We used the three-dimensional TEMPEST code to simulate the AN-101 pump jet mixing with a single 20-ft (6.1-m) off-center pump for nine baseline and inverted pump cases. The baseline pump has an intake below the injection nozzles and the inverted pump has injection nozzles below the pump inlet.

Table 5.1 shows the predicted solids erosion amount and average thickness of the solids layers that are not eroded for all nine cases. The table also presents the mixing time required to arrive at the final erosion conditions for these nine inverted pump cases.

Table 5.1. Predicted Erosion Amount of AN-101 Solids Layer by a Single Off-Centered Pump

Pump Type	Yield Strength, Pa	Pump Operation Time, min	Solids Erosion Amount, vol%	Remaining Solids Layer Thickness, in. (m)
Baseline Pump (intake below injection nozzles)	1	20	100	0
	5	40	100	0
	20	40	85.1	2.8 (0.072)
	60	40	80.1	3.8 (0.096)
	100	110	79.5	3.9 (0.098)
	150	120	78.6	4.0 (0.103)
Inverted Pump (injection nozzles below pump intake)	60	55	89.3	2.0 (0.051)
	100	75	86.1	2.6 (0.067)
	150	75	83.6	3.1 (0.079)

The AN-101 simulations indicated that the single 20-ft (6.1 m) off-center baseline mixer pump mobilized the expected waste solids, even those at the farthest tank wall, for all yield strengths (1, 5, 20, 60, 100, and 150 Pa). The baseline pump would mobilize 78.6 to 100% of the solids, depending on yield strength, of 1 to 150 Pa and 100% for yield strengths of 5 Pa or less. The smaller the yield strength, the greater will be the solids mobilization by the pump. On average, AN-101 waste solids with yield strengths above 20 Pa would not be eroded in the bottom 3–4 inches (0.07–0.1 m) of the tank.

A single 20-ft (6.1 m) off-center inverted, mixer pump would mobilize the solids at the farthest tank wall, eroding solids a little closer [average within 2–3 in. (0.05–0.08 m)] to the tank bottom than the baseline pump. The inverted pump would mobilize 83.6 to 89.3% of the AN-101 solids for the cases modeled with yield strengths of 60, 100, and 150 Pa. For yield strengths of 20 Pa or less, the inverted pump is expected to mobilize 100% of the solids.

As indicated in Table 5.1, a single 20-ft (6.1 m) off-center mixer pump (whether baseline pump or inverted pump) will mobilize the solids up to the farthest tank wall for yield strengths of 150 Pa or less. Because the yield strength of the expected AN-101 waste is estimated to be less than 150 Pa, the AN-101 pump mixing model results indicate that a single mixer pump would suffice to mobilize the bulk of the solids.

6.0 References

Allemann RT, ZI Antoniak, WD Chvala, LE Efferding, JR Friley, WB Gregory, JD Hudson, JJ Irwin, NW Kirch, TE Michener, FE Panisko, CW Stewart, and BM Wise. 1994. *Mitigation of Tank 241-SY-101 by Pump Mixing: Results of Testing Phases A and B.* PNL-9423, Pacific Northwest National Laboratory, Richland, WA.

Brewster ME, NB Gallagher, JD Hudson, and CW Stewart. 1995. *The Behavior, Quantity, and Location of Undissolved Gas in Tank 241-SY-101*. PNL-10681, Pacific Northwest National Laboratory, Richland, WA.

Felmy AR. 1995. "GMIN: A Computerized Chemical Equilibrium Program Using a Constrained Minimization of the Gibbs Free Energy: Summary Report." *Chemical Equilibrium and Reaction Models*. Soil Science Society of America, Special Publication 42.

Galbraith JD, RA Kirkbride, SD Estey, and NW Kirch. 2002. *Tank 241-AN-101 Transfer Pump Evaluation and Recommendation*. RPP-10136, Numatec Hanford Corp., Richland, WA.

Hedengren DC, KM Hodgson, WB Barton, CW Stewart, JM Cuta, and BE Wells. 2000. *Data Observations on Double-Shell Flammable Gas Watch List Tank Behavior*. RPP-6655 Rev. 0, CH2M HILL Hanford Group, Inc., Richland, WA.

Hedengren DC, TA Hu, MA Kufahl, DJ McCain, CW Stewart, JL Huckaby, LA Mahoney, and KG Rappe. 2001. *Data and Observations of Single-Shell Flammable Gas Watch List Tank Behavior*. RPP-7249, CH2M HILL Hanford Group, Inc., Richland, WA.

Herting DL. 1997. Results of Dilution Studies with Waste from Tank 241-AN-105. HNF-SD-WM-DTR-046 Rev. 0, Numatec Hanford Corp., Richland, WA.

Herting DL. 1998. Results of Dilution Studies with Waste from Tank 241-AN-104. HNF-3352 Rev. 0, Numatec Hanford Corp., Richland, WA.

Herting DL. 1999. Results of Dilution Studies with Waste from Tank 241-AW-101. HNF-4964 Rev. 0, Numatec Hanford Corp., Richland, WA.

Hudson JD, GS Barney, PR Bredt, AR Felmy, DL Herting, AP Larrick, DA Reynolds, CW Stewart, JM Tingey, and DS Trent. 1995. *An Assessment of the Dilution Required to Mitigate Hanford Tank 241-SY-101*. PNL-10417, Pacific Northwest National Laboratory, Richland, WA.

Johnson GD, NW Kirch, RE Bauer, JM Conner, CW Stewart, BE Wells, and JM Grigsby. 2000. *Evaluation of Hanford High-Level Waste Tank 241-SY-101*. RPP-6517 Rev. 0, CH2M HILL Hanford Group, Inc., Richland, WA.

Lambert SL. 1998a. *Tank Characterization Report for Double-Shell Tank 241-AN-103*. HNF-SD-WM-ER-702, Numatec Hanford Corporation, Richland, WA.

Lambert SL. 1998b. *Tank Characterization Report for Double-Shell Tank 241-SY-103*. WHC-SD-WM-ER-471, Numatec Hanford Corporation, Richland, WA.

Meyer PA and CW Stewart. 2001. *Preventing Buoyant Displacement Gas Release Events in Hanford Double-Shell Waste Tanks*. PNNL-13337, Pacific Northwest National Laboratory, Richland, WA.

Meyer PA, ME Brewster, SA Bryan, G Chen, LR Pederson, CW Stewart, G Terrones. 1997. *Gas Retention and Release Behavior in Double–Shell Waste Tanks*. PNNL-11536 Rev. 1, Pacific Northwest National Laboratory, Richland, WA.

Onishi Y and DS Trent. March 1999. "Mobilization Modeling of Erosion-Resisting Radioactive Tank Waste." *Proceedings of the Rheology in the Mineral Industry II*, Kahuku, Oahu, Hawaii. United Engineering Foundation, New York, pp. 45-56.

Onishi Y, KP Recknagle, and BE Wells. 2000. *Pump Jet Mixing and Pipeline Transfer Assessment for High-Activity Radioactive Wastes in Hanford Tank 241-AZ-102*. PNNL-13275, Pacific Northwest National Laboratory, Richland, WA.

Onishi Y, ST Yokuda, and CH Majumder. 2002. *Optimal Elevation and Configuration of Hanford's Double-Shell Tank Waste Mixer Pumps*. PNNL-13913, Pacific Northwest National Laboratory, Richland, WA.

Orme RM, DJ Geniesse, and GT MacLean. 2001. *Generalized Feed Delivery Description and Tank Specific Flowsheets*. RPP-8218 Rev. 0, CH2M HILL Hanford Group Inc., Richland, WA.

Stewart CW, JM Alzheimer, ME Brewster, G Chen, RE Mendoza, HC Reid, CL Shepard, and G Terrones. 1996. *In Situ Rheology and Gas Volume in Hanford Double-Shell Waste Tanks.* PNNL-11296, Pacific Northwest National Laboratory, Richland, WA.

Stewart CW, JD Hudson, JR Friley, FE Panisko, ZI Antoniak, JJ Irwin, JG Fadeff, LF Efferding, TE Michener, NW Kirch, and DA Reynolds. 1994. *Mitigation of Tank 241-SY-101 by Pump Mixing: Results of Full-Scale Testing*. PNL-9959, Pacific Northwest National Laboratory, Richland, WA.

Tingey JM, PR Bredt, and EH Shade. 1994. *The Effects of Heating and Dilution on the Rheological and Physical Properties of Tank 241-SY-101 Waste*. PNL-10198, Pacific Northwest National Laboratory, Richland, WA.

Wells BE, JM Cuta, SA Hartley, LA Mahoney, PA Meyer, and CW Stewart. 2002. *Analysis of Induced Gas Releases During Retrieval of Hanford Double-Shell Tank Waste*. PNNL-13782, Pacific Northwest National Laboratory, Richland, WA.

Distribution

No. of Copies

Offsite

M Katona
Dept. Civil/Environmental Engineering
Washington State University
Pullman, WA 99164

Onsite

3 DOE Richland Operations Office

JJ Davis (3)	S6-62

8 Numatec Hanford Company

SR Briggs	R3-47
PJ Certa	L4-07
JD Galbraith (3)	R3-73
CA Rieck (3)	S0-11

No. of Copies

6 CH2M HILL Hanford Group

JE Van Beek (3)	R3-47
EW Martinen (3)	R3-47

37 Pacific Northwest National Laboratory

GH Beeman	K9-09
SQ Bennett	K7-90
WF Bonner	K9-14
JR Bontha	K6-24
JW Brothers	K7-15
TM Brouns	K9-09
WL Kuhn	K7-15
DE Kurath	P7-28
Y Onishi (20)	K7-15
WC Weimer	K9-09
BE Wells (3)	K7-15
ST Yokuda (3)	K7-15
Information Release (2)	K1-06